UNIVERSIDAD DE CHILE
FACULTAD DE CIENCIAS QUÍMICAS Y FARMACÉUTICAS
Escuela de Postgrado

"NOVEL PLAYERS OF MITOCHONDRIAL COMMUNICATION WITH LYSOSOME AND ENDOPLASMIC RETICULUM"

Tesis para optar al grado de Doctor en Bioquímica por:

PABLO ANDRES RIVERA MEJÍAS

Director de tesis:
Dr. Sergio Lavandero González

Santiago, Chile, 2020

UNIVERSIDAD DE CHILE
FACULTAD DE CIENCIAS QUÍMICAS Y FARMACÉUTICAS

INFORME DE APROBACIÓN DE TESIS DE DOCTORADO

Se informa a la Dirección de la Escuela de Graduados de la Facultad de Ciencias Químicas y Farmacéuticas que la Tesis de Doctorado presentada por el candidato:

PABLO ANDRES RIVERA MEJÍAS

Ha sido aprobada por la Comisión de Evaluadora de Tesis como requisito para optar al grado de Doctor en Bioquímica, en el examen público rendido el día _____

Director de Tesis:

Dr. Sergio Lavandero González _____

Comisión Evaluadora de Tesis:

Dr. Verónica Eisner Sagues _____

Dr. Hugo Verdejo Pinochet _____

Dr. Alfonso Paredes Vargas _____

Dedicada a Jimena y mis padres

AGRADECIMIENTOS

A todos los que han estado en los momentos bajos y de fracaso durante este proyecto, tanto en Chile como en Alemania. A los que ayudaron a mantener la cordura y los ánimos cuando todo se veía sin alguna salida. A los que nunca les va importar en que revista publicaste y si tus datos calzan o no en la moda científica imperante. A los que estuvieron para tomarse una cerveza, para simplemente escuchar o no se incomodaron cuando no había ánimos ni siquiera para decir alguna palabra. A todos ellos los llamo los esenciales. Esa es mi principal lección de mi doctorado, no hay éxito ni felicidad sin tus esenciales.

FINANCIAMIENTO

Este trabajo contó con el financiamiento de la Agencia Nacional de Investigación y Desarrollo (ANID), Chile a través de los siguientes instrumentos

- Beca CONICYT Doctorado 64859 (P. Rivera).
- Proyecto FONDAP 15130011 (S. Lavandero)
- Proyecto FONDECYT 1161156 (S. Lavandero)
- Proyecto FONDECYT 1200490 (S. Lavandero)

PUBLICACIONES Y DIFUSIÓN DEL CONOCIMIENTO:

Publicaciones

- Sotomayor C*, **Rivera-Mejias P*,** Vasquez-Trincado C, López-Crisosto C, Morales PE, Pennanen C, Polakovicova I, Aliaga-Tobar V, Garcia L, Roa JC, Rothermel BA, Maracaja-Coutinho V, Ho Xua H, Meister G, Chiong M, Ocaranza MP, Corvalan AH, Parra V#, Lavandero S#. Angiotensin-(1-9) prevents cardiomyocyte hypertrophy by controlling mitochondrial dynamics via miR-129-3p/PKIA pathway. Cell Death Differentiation (in press, 2020). ISI: 8,1. Top 10 journal (RNK 27/299). *Shared first authorship. #Shared senior authorship. doi: 10.1038/s41418-020-0522-3. PMID: 32152556

- **Rivera-Mejías P**, Narbona-Perez AJ, Nolte H, Lampe P, Lavandero S, Langer T. OMA1 sustains cell viability under DNA-damaged induced by loss of lysosomal acidification. (MS in preparation)

Estadías de investigación en el extranjero:

Max Planck Institute for Biology of Aging. Langer Department. 2017-a la fecha

TABLE OF CONTENTS

TABLE OF FIGURES 8
ABBREVIATIONS 10
SUMMARY 13
INTRODUCTION 16
Chapter I: mitochondria-lysosome communication 16
Chapter II: Mitochondria-ER communication in cardiac hypertrophy 21
HYPOTHESIS 23
MAIN OBJECTIVE 23
SPECIFIC OBJECTIVES 23
MATERIALS AND METHODS 24
Generation and culture of cell lines 26
Treatments and immunoblotting 27
Oxygen consumption rate and extracellular acidification rate analysis 28
Cell death assay 28
Metabolomics and labelling experiments 28
Cardiomyocyte culture 29
Evaluation of cardiomyocyte hypertrophy 29
Assessment of mitochondrial calcium 30
Transmission electron microscopy 30
Quantification and statistical analysis 30
RESULTS 31
Chapter I 31
Chapter II 57
DISCUSSION 62
Chapter I 62
Chapter II 65
OPEN QUESTIONS 66
CONCLUSIONS 68
BIBLIOGRAPHY 70

TABLE OF FIGURES

Figure 1. Baf A1 treatment affects cell viability and OMA1 protects against cell death. 32
Figure 2. Loss of lysosomal acidification induces cell death in late time points independently of the concentration. 33
Figure 3. OMA1 prevents caspase dependent cell death induced by decrease of lysosomal acidification. 34
Figure 4. OMA1 prevents apoptotic cell death induced by loss of lysosomal acidification. 35
Figure 5. OMA1 prevents activation of the caspase pathway under loss of lysosomal acidification. 36
Figure 6. Autophagy inhibition does not induce cell death in neither WT nor OKO cells. 37
Figure 7. Lysosomal protease inhibitor does not induce cell death neither WT nor OKO cells 38
Figure 8. OMA1 prevents apoptosis activation induced by loss of lysosomal acidification. 39
Figure 9. OMA1 protects against cell death induced by loss of lysosomal acidification. 39
Figure 10. Loss of lysosomal acidification does not induce OPA1 processing. 40
Figure 11. Loss of lysosomal acidification does not affect OCR or ECAR in early time points. 41
Figure 12. Loss of lysosomal acidification decrease respiration in late time points. 42
Figure 13. Loss of lysosomal acidification does not affect extracellular acidification in late time points. 43
Figure 14. Effect of loss of lysosomal acidification over amino acids homeostasis. 45
Figure 15. Scheme of glutamine oxidative and reductive metabolism measured with uniformly labelled ^{13}C-Glutamine (U-^{13}C-Glutamine). 47
Figure 16. Fractions of glutamine incorporation into TCA metabolites. 48
Figure 17. Glutamine incorporation into TCA cycle metabolites. 50
Figure 18. Loss of lysosomal acidification decrease SDHA and SDHB protein levels. 51
Figure 19. Loss of lysosomal acidification induces the iron starvation response. 52
Figure 20. Iron supplementation partially rescues respiration. 53
Figure 21. Iron supplementation partially rescues OCR parameters. 54
Figure 22. Iron supplementation rescues iron-sulfur cluster binding protein levels and Caspase-3 activation. 55
Figure 23. Iron supplementation rescues cell death induced by loss of lysosomal acidification. 56

Figure 24. Angiotensin-(1-9) treatment prevents cardiomyocyte hypertrophy induced by NE..... 58
Figure 25. Angiotensin-(1-9) treatment induces mitochondrial elongation and prevents mitochondrial fragmentation induced by NE. 58
Figure 26. Angiotensin-(1-9) treatment keeps mitochondrial-ER communications and prevents the activation pro-hypertrophic signalling pathway. 60
Figure 27. Model of mitochondria-lysosome communication 69
Figure 28. Model mitochondria-ER communication 69

ABBREVIATIONS

AA: Antymicin A

Ang-(1-9): Angiotensin-(1-9)

ANOVA: Analysis of variance

AT2R: Angiotensin type 2 receptor

ATP: Adenosine triphosphate

Baf A1: Bafilomycin A1

BECN1: Beclin 1

Casp3: Caspase-3

c-CASP3: Cleaved Caspase-3

CcO: Cytochrome c Oxidase

Con A: Concanamycin A

C-PARP: cleaved PARP

DFP: Deferiprone

DMEM: Dulbecco's modified eagle medium

DNA: Deoxyribonucleic acid

DRP1: Dynamin related protein 1

ECAR: Extra cellular acidification rate

EM: Electron microscopy

ER: Endoplasmic reticulum

ERMES: ER-mitochondria encounter structures

esiRNA: Endoribonuclease-prepared siRNAs

ETC: Electron transport chain

FACS: Fluorescence-activated cell sorting

FBS: Fetal bovine serum

FC: Fold changes

FCCP: Carbonyl cyanide-4-(trifluoromethoxy)phenylhydrazone

IMM: Inner mitochondrial membrane

IMS: Intermembrane space

KD: *Knock down*

KO: *Knock out*

LD: Lipid droplets

L-OPA1: Long OPA1

MCU: Mitochondrial calcium uniporter

MEF: Mouse embryonic fibroblast

MFF: Mitochondrial fission factor

Mfn1: Mitofusin 1

Mfn2: Mitofusin 2

MID49: mitochondrial dynamics protein 49

MID51: mitochondrial dynamics protein 51

MPC: Mitochondrial pyruvate carrier

NDUFS1: NADH-ubiquinone oxidoreductase 75 kDa subunit

NE: Norepinephrine

OCR: Oxygen consumption rate

OKO: OMA1 *Knock out*

Olig: Oligomycin

OMA1: Overlapping with the m-AAA protease 1

OMM: Outer mitochondrial membrane

OPA1: Optic atrophy protein 1

OXPHOS: Oxidative phosphorylation

PARP: Poly (ADP-ribose) polymerase

PHB2: Prohibitin 2

PI: Proteases inhibitors

RAS: Renin Angiotensin system

RCAN1.4: Regulator of Calcineurin 1 Isoform 4 (RCAN1.4)

ROI: Region of interest

Rot: Rotenone

SDHA: Succinate dehydrogenase subunit A

SDHB: Succinate dehydrogenase subunit B

S-OPA1: Short OPA1

TCA: Tricarboxylic acid cycle

TfR: Transferrin receptor

ULK1: Unc-51 like autophagy activating kinase 1

Vclamps: vacuolar and mitochondrial patch

WT: *Wild type*

YME1L: Yeast mitochondrial DNA scape like-1

SUMMARY

Background: Mitochondria fulfil several functions that are essential for cellular homeostasis. This organelle forms a dynamic network, whose morphology is controlled by a set of GTPases dynamin-like proteins at the outer mitochondrial membrane (OMM) and inner mitochondrial membrane (IMM). In the IMM, the fusion process is mediated by OPA1. The activity of this pro-fusion protein is regulated, at least in part, by the mitochondrial metallo-protease OMA1. Loss of OMA1 prevents the processing of OPA1 and cell death induced by different stress conditions, indicating that OMA1 has mainly a pro-apoptotic function. Mitochondria interacts physically and functionally with other organelles, including lysosomes and endoplasmic reticulum (ER). Several studies in yeast and mammalian cells shown that vacuole/lysosomal dysfunction impairs mitochondrial homeostasis, via an unknown mechanism. Similarly, mitochondrial dysfunction impair lysosomal homeostasis, showing the bi-directional communication and the necessity to prevent damage of at least of one of these organelles during mitochondria/lysosome dysfunction. Mitochondria-ER communication plays an important role in cardiac pathophysiology. Norepinephrine (NE) treatment induces mitochondrial fragmentation and reduces mitochondria-ER communication, leading to the activation of calcineurin, a pro-hypertrophic cytosolic protein. Angiotensin-(1-9) is a nine amino peptide, member of the non-canonical renin-angiotensin system, with anti-hypertrophic properties *in-vitro* and *in-vivo.* However, the mechanism of action of angiotensin-(1-9) remains unknown.
Hypothesis: “OMA1 prevents mitochondrial dysfunction and cell death induced by loss of lysosomal acidification” and “angiotensin-(1-9) treatment prevents the loss mitochondria-ER communication during cardiomyocyte hypertrophy”.
Aims: To study the effect of loss of lysosomal acidification on mitochondrial homeostasis and the effect of angiotensin-(1-9) treatment over mitochondria-ER communication.

Results: First, to address the effect of loss of lysosomal acidification over mitochondrial homeostasis, mouse embryonic fibroblast (MEF) wild type (WT) and OMA1 knockout (OKO) cells were treated with the V-ATPase inhibitor Bafilomycin A1 (Baf A1). Loss of lysosomal acidification induces cell death in WT, but more strongly in OKO cells, suggesting that OMA1 was required for cell viability under these experimental conditions. Nevertheless, the inhibition of early steps of autophagy did not affect cell viability, indicating that the effect of Baf A1 over cell death was independent of autophagy. Baf A1 reduced oxygen consumption rate (OCR) and glutamine incorporation into the tricarboxylic acid cycle (TCA) cycle in WT and OKO cells. OMA1 loss increased glutamine the incorporation into the TCA cycle. Loss of lysosomal acidification reduced iron availability, inducing an iron starvation response and reduction of iron-sulfur cluster binding proteins. Iron supplementation rescues respiration, iron-sulfur cluster binding protein levels and cell viability, indicating that iron is the main mediator of lysosome-mitochondria communication. Second, to address the effect of angiotensin-(1-9) over mitochondria-ER communication, neonatal rat cardiomyocytes were treated with NE in presence or absence of angiotensin-(1-9). This peptide prevented cardiomyocyte hypertrophy, mitochondrial fragmentation and loss of mitochondria-ER communication. Interestingly, angiotensin-(1-9) treatment by itself stimulated mitochondrial elongation and increased mitochondrial calcium buffer capacity. Finally, angiotensin-(1-9) treatment prevented the activation of Calcineurin/NFAT pathway triggered by NE, suggesting that this peptide regulates cytosolic calcium signalling.

Conclusions. OMA1 plays a pro-survival role in conditions of V-ATPase inhibition and regulates glutamine incorporation into TCA cycle. Loss of lysosomal acidification impairs mitochondrial homeostasis by reducing iron availability, suggesting that iron plays a key role in lysosome-mitochondria communication. Angiotensin-(1-9) treatment prevents cardiomyocyte hypertrophy, mitochondrial fragmentation and loss of mitochondria-ER communication induced by NE. Angiotensin-(1-9) anti-hypertrophic

mechanism involves the regulation of cytosolic calcium signalling, probably by keeping mitochondria-ER functional communication

INTRODUCTION

Chapter I: mitochondria-lysosome communication

Mitochondria fulfil several key functions for cellular homeostasis. Traditionally called “the powerhouse of the cell” due to its role in ATP production, this organelle also participates in other essential pathways such as apoptotic cell death, inflammation, biosynthetic pathways, calcium signalling, lipid homeostasis, etc. **(1)**. Mitochondria is a double-membrane bound organelle, with different compartments where several biochemical reactions are carried on. Between the outer mitochondrial membrane (OMM) and the inner mitochondrial membrane (IMM), there is the intermembrane space (IMS). The IMM delimits the mitochondrial matrix and forms an additional compartment called cristae, that harbours the protein complexes necessary for oxidative phosphorylation (OXPHOS) and ATP production **(2)**.

Against the traditional “text book” view of mitochondria, advances in microscopy techniques allow us to see the real and more complex organisation of this organelle. Mitochondria form a dynamic network, which morphology, biogenesis, turnover and distribution changes in response to cellular requirement and stress conditions **(3, 4)**. Mitochondrial morphology is tightly regulated by a set of dynamin-like proteins with GTPase activity in the OMM and IMM.

The fusion process in the OMM is regulated by the dynamin-like proteins mitofusin 1 (Mfn1) and mitofusin 2 (Mfn2). Mitofusins are anchored into the OMM via its C-terminal transmembrane domains, mediating fusion via homo or heterotypic interactions of two adjacent mitochondrial membranes **(5)**. Additionally, Mfn2 mediates the tethering between the endoplasmic reticulum (ER) and mitochondria. However, this function is still under debate **(6, 7)**.

The main regulator of OMM fission is the cytosolic resident dynamin-like protein 1 (DRP1) **(8)**. The dynamic localization of DRP1 is tightly regulated by a set of post-translational modifications that includes phosphorylation, acetylation and sumoylation **(9)**. After being targeted into the mitochondrial fission sites, DRP1 interacts with adaptor proteins in the OMM, such as the mitochondrial fission factor (MFF), mitochondrial fission protein (Fis1) or mitochondrial dynamics proteins 49 and 51 kDa (MID49 and MID51) **(2)**. Moreover, several studies have reported that ER tubes and actin filaments provide the mechanical force necessary for the scission of the OMM and IMM **(10-14)**.

The GTPase optic atrophy protein 1 (OPA1) regulates the fusion of the IMM. OPA1 exits in multiple forms generated by alternative splicing and proteolytic cleavage **(1)**. In humans, at least eight isoforms can be synthetized via alternative splicing, given rise to the long OPA1 forms (L-OPA1) **(15)**. L-OPA1 forms are anchored to the IMM with their catalytic site facing the IMS **(16)**. These membrane-bound long forms are processed at basal and stress conditions by two IMS proteases: yeast mitochondrial DNA scape like-1 (YME1L) and overlapping with *m*-AAA (OMA1) proteases **(17)**. The processing by these two proteases generates the OPA1 soluble short forms (S-OPA1). Recent reports have shown that L-OPA1 forms are necessary and sufficient for mitochondrial fusion **(18, 19)**, so its proteolytic cleavage limits its activity and represents an important regulatory mechanism to balance mitochondrial dynamics **(17)**.

OMA1 is an ATP-independent zinc-metalloprotease from the M48 family **(20)**. This protein was first described in yeast, where possesses overlapping functions with m-AAA proteases due to its capacity to degrade a thermo-sensitive form of the IMM insertase OXA1 **(21)**, a protein that participates in mitochondrial protein import and insertion. Also in yeast, OMA1 mediates the selective degradation of Cox1, part of the cytochrome c oxidase complex (CcO), when cells lack the assembly factor Coa2 **(22)**.

In mammals, OMA1 has been characterized as a stress-activated protease, mediating the cleavage of OPA1, then regulating mitochondrial dynamics and ultrastructure **(23, 24)**. Several stressors such as loss of the m-AAA protease AGF3L2 **(25)**, loss of the mitochondrial scaffold protein Prohibitin-2 (PHB2) **(26)**, YME1L deletion **(27)**, loss of mitochondrial membrane potential, hypoxia, heat stress, among others **(23)** can activate OMA1. Although it is difficult to define which one is the signal that OMA1 senses, some studies proposed a sensing domain in OMA1 structure, which is necessary for its activation. OMA1 is inserted in the IMM with its catalytic domain (C-terminal) facing the IMS and the N-terminal facing the mitochondrial matrix. OMA1 is constitutively active, but its activity is enhanced in the presence of a stress signals. This increase in OMA1 activity depends on a N-terminal stress-sensor domain **(23)**. However, a study in yeast proposed that OMA1 activation depends on a domain localized in the C-terminal region **(28)**. Despite its constitutive activity, the loss of OMA1 induces a mild or no phenotype in-vivo. Whole body *Knock Out* (KO) model only showed a defect on thermogenesis that led to a mild weight increase **(20)**. Other studies showed that the deletion of OMA1 in heart **(27, 29)** or brain **(26, 30)** does not induce any phenotype, suggesting that OMA1 plays a role just under stress-related conditions.

Activation of the intrinsic apoptotic pathway involve the loss of *cristae* junctions and mitochondrial fragmentation **(31)**, leading to cytochrome c release (previous OMM permeabilization) and apoptosis activation **(32)**. L-OPA1 plays a central role in the apoptotic pathway, maintaining cristae junctions and mitochondrial fusion **(32, 33)**. Under stress conditions, OPA1 is cleaved by OMA1, inhibiting mitochondrial fusion as an initial compensatory response. Nevertheless, if the stress persist, this can lead to cell death. Cardiac-specific deletion of YME1L induces severe heart failure, related with an increase of mitochondrial fragmentation and OPA1 processing, phenomenon prevented by the deletion of OMA1 **(27)**. Supporting this, the cardiomyocyte-specific deletion of OMA1 prevents heart failure induced by Isoproterenol, angiotensin

II or transverse aortic constriction (TAC) **(29)**. In kidney, loss of OMA1 protects against acute kidney injury induced by ischemia **(34)**. Altogether, these data show that OMA1 has a pro-apoptotic function under stress and its deletion is a reliable strategy to prevent mitochondrial dysfunction and cell death.

Additionally to the dynamic regulation of its morphology and activity, mitochondria interacts physically and functionally with other organelles, interactions that are fundamental to sustain mitochondrial homeostasis and cell viability. Mitochondrial interacts with ER, peroxisomes, Golgi apparatus, lipid droplets (LD), melanosomes and lysosomes **(35)**.

Lysosome-mitochondria communication has been mainly characterized in the baker yeast *Saccharomyces cerevisiae*. The vacuolar (lysosomes in mammals) and mitochondrial patch (vCLAMPs), term given to the mitochondria-vacuole contact sites, are essential for mitochondrial homeostasis under the loss of ERMES (ER-mitochondria encounter structures) **(36, 37)**. Loss of ERMES increases the area of vCLAMPs, and conversely, loss of vCLAMPs components increase the number of ERMES. The loss of both structures is lethal **(37)**. vCLAMPs serves as an alternative pathway for phospholipid transport, sustaining lipid supply under loss of ERMES **(37).** Importantly, the solely loss of one of these pathways does no induces a strong mitochondrial phospholipid phenotype.

Mitochondrial dysfunction is a hallmark of aging, being considered a target and contributor of this process **(38)**. Nevertheless, the mechanism that explain the decline of mitochondrial function during aging is yet not fully understood **(39)**. An overexpression screening in *Saccharomyces cerevisiae* shows that loss of vacuole acidification precedes mitochondrial fragmentation and dysfunction during aging. Interestingly, preventing the decline of vacuole acidification suppresses mitochondrial dysfunction and extends lifespan **(40)**. Additionally, the direct V-ATPase inhibition (proton pump that keeps vacuolar acidification) is sufficient to induce mitochondrial fragmentation and dysfunction,

independently of aging and autophagy, showing the central role of vacuolar homeostasis on mitochondrial function. However, the mechanism of how loss of vacuolar acidification induces mitochondrial dysfunction remains unclear. A similar correlation has been reported in human pathologies associated to lysosomal dysfunction. Evidence of mitochondrial dysfunction, including respiration defects and morphological abnormalities, is observed in several experimental models of lysosomal storage diseases, including Guacher´s disease and Niemann-Pick disease type C **(41)**. However, similar as in yeast, the mechanism that explain this correlation remains elusive.

Interestingly, several groups have reported that mitochondrial dysfunction impairs lysosomal homeostasis, showing the bidirectional relationship between both organelles. Loss of apoptosis induced factor (AIF), necessary for ETC function, OPA1 or PINK1 (involved in mitophagy) in MEF cells **(42)**, UQCRC1 *knock down* in Hela cells (subunit of respiratory chain complex III) **(43)**, or TFAM deletion in CD4(+) T lymphocytes **(44)**, disrupts lysosomal homeostasis. This interdependence depicts the importance of prevent the damage of, at least, one of these organelles during mitochondrial/lysosomal dysfunction. As we described previously, OMA1 has shown in several experimental models to be a powerful tool to prevent mitochondrial dysfunction and cell death, making it an attractive target in conditions of lysosomal dysfunction.

Thus, the question that we will address in this chapter is:

- How loss of lysosomal acidification induce mitochondrial dysfunction in mammalian cells?
- Does OMA1 deletion prevents mitochondrial dysfunction and cell death under loss of lysosomal acidification?

Chapter II: Mitochondria-ER communication in cardiac hypertrophy

As in yeast, mammalian mitochondria-ER contact sites serve as platforms for metabolites exchange. Lipid exchange and calcium transfer from ER to mitochondria establish a functional interaction between both organelles. Calcium transfer is fundamental for mitochondrial homeostasis and cell fate, regulating, for example, bioenergetics and cell death **(45)**. Mitochondrial calcium uptake is mediated by an IMM complex formed by the mitochondrial calcium uniporter (MCU) **(46, 47)**, together with the regulatory sub-units MICU1 and MICU2 **(48)**. This complex act as a gatekeeper, being insensitive to low calcium concentrations. ER- mitochondria contact sites serve as a high-calcium concentration microdomains that allows the efficient transport of this ion **(49-51)**.

Mitochondria play a key role in myocardial function due to the high energetic demand during contraction. The onset and progression of several cardiac pathologies are associated with a decline of mitochondrial homeostasis **(3)**. However, the direct role of mitochondria-ER communication in cardiac pathologies is less clear. Electric or pharmacological stimulation of ER calcium release, leads to a subsequent increase of mitochondrial calcium levels in cardiomyocytes **(52-54)**. Interestingly, regulation of MCU levels in cardiomyocytes, results in opposite effects in the amplitudes of spontaneous cytosolic calcium peaks, suggesting the modulation of cytosolic calcium levels by mitochondrial uptake **(55)**.

Cardiac hypertrophy involves structural, morphological and functional changes of cardiomyocytes, in response to variety of stimuli, including ischemia and neurohormonal stimulation. Cardiomyocyte hypertrophy begins as a compensatory response in order normalized wall stress and oxygen demand **(56)**. However, chronical conditions can lead to the development of pathological hypertrophic growth, cell death and finally heart failure **(57)**. In our previous work, we described that the onset of cardiomyocyte hypertrophy

involves the loss of mitochondria-ER communication and mitochondrial fragmentation. In a model of neonatal cardiomyocytes, the pro-hypertrophic treatment norepinephrine (NE), reduced mitochondrial calcium uptake stimulated by histamine and mitochondrial-ER contacts **(58)**. In an additional study, we described that NE treatment induces mitochondrial fragmentation, via a mechanism depended of Calcineurin, a cytosolic resident protein that is activated under increase of cytosolic calcium levels **(59)**. These results indicates that the loss of mitochondria-ER communication under NE treatment could leads to the increase of cytosolic calcium signalling, resulting in the development of cardiomyocyte hypertrophy. Thus, interventions that helps to preserves mitochondria-ER communication can be novel therapeutic strategies to prevent pathological cardiac hypertrophy.

Angiotensin-(1-9) (Ang-(1-9)) is a nine-amino acid peptide, member of the non-canonical renin-angiotensin system (RAS), produced by the hydrolysis of angiotensin I **(60)**. Ang-(1-9) interacts with the angiotensin II (Ang II) type 2 receptor (AT2R), to counteract the actions of the classical RAS signaling, mediated mainly by Ang II/AT1R signaling axis **(61)**. *In-vitro* and *in-vivo* studies showed that Ang-(1-9) prevents cardiac hypertrophic in response to either Ang II or NE **(62, 63)**. However, up to the date, no mechanism is known for Ang-(1-9) anti-hypertrophic effect.

Thus, the aim of this chapter is to study the regulation of mitochondria-ER communication and mitochondrial morphology by Ang-(1-9) treatment in neonatal cardiomyocytes.

HYPOTHESIS

“Loss of OMA1 prevents mitochondrial dysfunction and cell death induced by loss of lysosomal acidification” and “Ang-(1-9) treatment prevents the loss mitochondria-endoplasmic reticulum communication during cardiomyocyte hypertrophy”

MAIN OBJECTIVE

To study the effect of loss of lysosomal acidification on mitochondrial homeostasis and the effect of Angiotensin-(1-9) treatment over mitochondria-ER communication

SPECIFIC OBJECTIVES

Chapter I

A. To evaluate the effect of loss of lysosomal acidification on cell viability in WT and OMA1 KO MEF cells.
B. To characterize the effects of loss of lysosomal acidification over mitochondrial homeostasis in WT and OMA1 KO MEF cells.
C. To determine the mechanism associated to cell viability changes in WT and OKO MEF cells when lysosomal acidification is inhibited.

Chapter II

A. To evaluate the effect of Ang-(1-9) treatment over mitochondria-ER communication and mitochondrial morphology, in cultured cardiomyocyte treated with NE.

MATERIALS AND METHODS

Reagents

Reagent or resource	Source	Identifier
Antibodies		
PARP	Cell Signalling Technologies	Cat#9542, RRID: AB_2160739
OPA1	BD Biosciences	Cat# 612606, RRID:AB_399888
Cleaved Caspase-3 (Asp175)	Cell Signaling Technology	Cat# 9661, RRID:AB_2341188
LC3B	Sigma-Aldrich	Cat# L7543, RRID:AB_796155
β-Actin	Sigma-Aldrich	Cat# A5441, RRID:AB_476744
ULK1	Cell Signaling Technology	Cat# 8054, RRID:AB_11178668
BECN1	Cell Signaling Technology	Cat# 3495, RRID:AB_1903911
p62	Novus	Cat# H00008878-M01, RRID:AB_548364
SDHA	Abcam	Cat# ab14715, RRID:AB_301433
NDUFS1	Abcam	Cat# ab169540 , RRID: AB_2687932
SDHB	Abcam	Cat# ab14714, RRID:AB_301432
Transferrin receptor	Santa Cruz	Cat# sc-65882 RRID: AB_1120670
Chemical, peptides and recombinant proteins		
DMEM, high glucose, GlutaMAX™ Supplement	Gibco	Cat#61965026

Sodium Pyruvate (100 mM)	Gibco	Cat#11360070
MEM Non-Essential Amino Acids Solution (100X)	Gibco	Cat#11140050
Bafilomycin A1	Santa Cruz Biotechnology	Cat#sc-201550A
Concanamycin A	Santa Cruz Biotechnology	Cat#sc-202111
DMSO	Sigma-Aldrich	Cat#D2650-5X5ML
Fetal Bovine Serum (FBS)	Sigma-Aldrich	Cat# F7524, lot:BCBW9645
Penicillin-Streptomycin	Gibco	Cat#15140122
DMEM powder	Sigma-Aldrich	Cat#D5030-10X1L
D-(+)-Glucose	Sigma-Aldrich	Cat#G7021
L-Glutamine (200 mM)	Gibco	Cat#25030081
Iron(III) citrate	Sigma-Aldrich	Cat# F6129
YOYO™-1 Iodide	Invitrogen	Cat#Y3601
SiR-DNA kit	SpiroChrome	Cat#SC007
Carbonyl cyanide 3-chlorophenylhydrazone (CCCP)	Sigma-Aldrich	Cat#C2759
Z-VAD-FMK	Santa Cruz Biotechnology	Cat#sc-3067
Lipofectamine™ RNAiMAX	Invitrogen	Cat#13778075
L-Glutamine-$^{13}C_5$	Sigma-Aldrich	Cat#605166
Dialyzed FBS	Gibco	Cat# 26400044
E-64d	Sigma-Aldrich	Cat# E8640
Pepstatin A	Sigma-Aldrich	Cat# P5318
Angiotensin-(1-9)	GL Biochem Ltd	
Norepinephrine	Sigma-Aldrich	A0937
Commercial Assays		
Bio-Rad Protein Assay Dye Reagent Concentrate	Bio-Rad	Cat#5000006

Magic Red™ Cathepsin B Kit	Bio-Rad	Cat#ICT938
Seahorse XF Cell Mito Stress Test Kit	Agilent	Cat#103015-100
Seahorse XFe96 FluxPak	Agilent	Cat#102416-100
NucView® 488 and RedDot™ 2 Apoptosis and Necrosis Kit	Biotium	Cat#30072
Experimental models: Cell lines		
Mouse embryonic fibroblast	Dr. Thomas Langer	N/A
Oligonucleotides		
esiRNA ULK1	Sigma-Aldrich	Cat#EMU044591
esiRNA BECN1	Sigma-Aldrich	Cat#EMU069661
Software and Algorithms		
Image J	Schneider et al., 2012	https://imagej.net/ImageJ1
Instant Clue	Nolte et al., 2018	http://www.instantclue.uni-koeln.de/download.html

Generation and culture of cell lines

Oma1loxP/loxP conditional mice were generated by ESC targeting using pRapidFlirt constructs designed to insert intronic LoxP sites flanking exon 3 of Oma1 **(17)**. Primary fibroblasts were isolated from Oma1loxP/loxP, embryonic day 13.5 embryos and immortalized using a plasmid encoding SV40 large T antigen. Immortalized fibroblasts were transduced with recombinant His-TAT-NLS-Cre (HTNC) fusion protein (4 µM), incubated for 20 h, washed with PBS, and supplemented with growth medium. Individual clones were sorted by flow cytometry into 96-well plates (FACS Aria III; BD) using the FASC DIVA software (BD), expanded, and subsequently genotyped for deletion of Oma1 by PCR and immunoblotting **(17)**. Cells were cultured at 37°C (humidified, 5%

CO_2 [vol/vol]) in DMEM-GlutaMAX supplemented with 10% (v/v) FBS, 1 mM sodium pyruvate, and nonessential amino acids.

Treatments and immunoblotting

For cell death experiments, 125.000 cells per well were seeded in 6-well plates (day 1). After 24 h incubation, the media was replaced by fresh culture media containing DMSO or Baf A1 (5 nM), Concanamycin A (1 or 5 nM) or Iron citrate (50 µM), depending on the experimental design (day 2). After 24 h incubation, cells were rinsed twice with cold PBS and stored at -80°C up to the day of extraction. For *knock down* experiments, 300.000 cells per well were seeded in the morning day of transfection. During the afternoon of the same day, cells were transfected with esiRNA at the final concentration of 1000 ng per well using Lipofectamine RNAiMAX, following manufacturer's protocol. After 24 h incubation, the lipofectamin-containing media was replaced for fresh media. After 72 h, cells were rinsed twice with cold PBS and stored at -80°C up to the extraction day. For protein extraction, frozen cells were lysed in RIPA buffer [50 mM HEPES/NaOH, pH 7.5, 150 mM NaCl, 1 mM EDTA, 1.0% (v/v) Triton X-100, 0.1% (w/v) SDS, 0.5% (w/v) sodium deoxycholate, protease inhibitor cocktail (Roche)], harvested and incubated for 10 min on ice. After that, the cell lysates were centrifuged at 16,000 g for 10 min at 4°C and the supernatant transferred to 1.5 ml Eppendorf tubes. Protein concentration was determined utilizing Bio-Rad Protein Assay Dye Reagent. 50 µg of protein per sample were resolved by tris-glycine or tris-tricine (OPA1) SDS-page, transferred to nitrocellulose membranes, and subjected to immunoblotting using the following antibodies: PARP (1:1.000), OPA1 (1:2.000), c-Caspase 3 (1:500), LC3B (1:2.000), β-Actin (1:5.000), ULK1 (1:1.000), BECN1 (1:1.000), p62 (1:2.000), SDHA (1:5.000), SDHB (1:1.000), NDUFS1 (1:2.000) and TfR(1:1.000) .

Oxygen consumption rate and extracellular acidification rate analysis

Oxygen consumption rate (OCR) and extracellular acidification rate (ECAR) were measured with a Seahorse XFe96 Analyzer (Agilent). For 8 h Baf A1 treatment experiments, 30.000 cells per well were plated one day before the assay. For 16 h Baf A1 treatment experiments, 5.000 cells per well were plated two days before the assay. For these experiments, we used Oligomycin (2 µM), FCCP (0,5 µM) and Antimycin A and rotenone (0,5 µM) as final concentrations. The OCR and ECAR values were normalized to total amount of protein per well. Oxygen consumption parameters were obtained utilizing the Seahorse Wave Desktop Software.

Cell death assay

For the cell death assay experiments, we utilized an Essen-Bioscience IncuCyte S3 microscope that allowed us to keep the cells in normal cell culture conditions. For these experiments, 5.000 cells per well were plated in 96-well plates. After 24 h, the media was replaced for media containing the treatments plus YOYO-1(0,5 µM) and SirDNA (0,5 µM). YOYO-1 positive objects (death cells) and SirDNA positive objects (total cell number) were analysed every 2-6 h for a total of 24 h. For flow cytometry experiments, we treated cells for 24 h and then we analysed cell populations stained with NucView® 488 (active caspase 3/7) and RedDot™ 2 (plasma membrane permeabilization) by FACS (FACS Aria III; BD Biosciences) flow cytometer.

Metabolomics and labelling experiments

For steady-state amino acids measurements, 125.000 cells per well were seeded in 6-well plates. The day after, the media was replaced for fresh media containing DMSO or Baf A1 (5 nM). After 16 h treatment, cells were rinsed twice with 0,1% NaCl and rapidly frozen in liquid nitrogen and stored at -80°C up to the extraction day. For labelling experiments, 125.000 cells per well were

plated in 6-well plates. The day after, the media was replaced for glutamine-free DMEM media containing 4 mM L-glutamine-$^{13}C_5$, 25 mM glucose, 10% dialized-FBS and sodium pyruvate plus DMSO or Baf A1 (5 nM). After 16 h treatment, cells were rinsed twice with 0,1% NaCl and quickly frozen in liquid nitrogen and stored at -80°C up to the extraction day. For intracellular metabolites extraction, we took the plates stored at -80°C and we added to each well 400 µl of extraction buffer (60% methanol, 20% acetonitrile, 20% H_2O). After 10 min of incubation at -20°C, the supernatant was collected and then, we added other 400 µl of extraction buffer. After that, cells were scrapped and collected. Later, samples were centrifuged at 16,000 g for 10 min at 4°C and the supernatants were transferred into 1.5 ml Eppendorf tubes and stored at -80°C. Metabolomics analysis were performed on a Thermo Fisher Q Exactive GC Orbitra GC-MS/MS.

Cardiomyocyte culture

Cardiomyocytes were isolated from hearts of neonatal Sprague-Dawley rats as described previously (13). Rats were bred at the University of Chile Animal Breeding Facility. Primary cell cultures were incubated with or without Ang-(1-9) (100 µM) and/or NE (10 µM) for 0–24 h in DMEM/M199 (4:1) medium, in the presence or absence of the various inhibitors and other genetic reagents. All studies conformed to the Guide for the Care and Use of Laboratory Animals published by the US National Institutes of Health (NIH Publication, 8th Edition, 2011) and were approved by the Ethics Review Committee from the Faculty of Chemical and Pharmaceutical sciences, University of Chile.

Evaluation of cardiomyocyte hypertrophy

Sarcomerization was observed with confocal microscopy (Carl Zeiss LSM 5, Pascal 5 Axiovert 200 microscope) of methanol permeabilized cells stained

with rhodamine-phalloidin (1:400; F actin staining). For the cellular perimeter and mitochondrial area analysis, one focal plane of at least 50 cells from randomly selected fields was analyzed using ImageJ software (NIH).

Assessment of mitochondrial calcium

To evaluate mitochondrial calcium levels, images were obtained from cultured cardiomyocytes preloaded with Rhod-FF (5.4 μM, 30 min). At the end of each measurement, 10 μM of CCCP was used as control. Measurements were performed in an inverted confocal microscope (Carl Zeiss LSM 5, Pascal 5 Axiovert 200 microscope).

Transmission electron microscopy

Cells were fixed in 2.5% glutaraldehyde in sodium cacodylate buffer, embedded in 2% agarose, post-fixed in buffered 1% osmium tetroxide and stained in 2% uranyl acetate, dehydrated with an ethanol graded series, and embedded in EMbed-812 resin. Thin sections were cut on an ultramicrotome and stained with 2% uranyl acetate and lead citrate. Images were acquired on a FEI Tecnai G2 Spirit electron microscope equipped with a LaB6 source and operating at 120 kV. Measurements of mitochondrial area, perimeter, circularity, and mitochondrial density were performed using the Multi Measure ROI tool in the ImageJ (NIH) software package.

Quantification and statistical analysis

Statistical analysis was performed with InstanClue 0.5.3. The data is represented as the media ± 95% confidence interval of, at least, three independent experiments. Two-way Anova was used to determined statistical significance and unpaired t-student for two group's comparison. p values are plotted in the figures, assuming statistical significance with $p<0.05$.

RESULTS

Chapter I

Our first aim was to address whether the loss of lysosomal acidification impairs mitochondrial and cellular homeostasis in mammalian cells. To this end, MEF *wild type* (WT) and OMA1 KO (OKO) cells were treated the endo-lysosomal V-ATPase inhibitor Baf A1 that impairs the acidification of these compartments **(64)**. We performed a cell death kinetic experiment during 32 h following the signal of YOYO-1, a cell impermeable nucleic acid fluorescent dye that binds DNA when the permeability of the plasma membrane is compromise, phenomenon that happens during late apoptosis or necrotic cell death **(65)**. In order to quantify the population of cells that are undergoing cell death, we additionally culture the cells with sir-DNA, a cell permeable nucleic acid dye that let us know the total cell number (death + live cells). Images of these cells were took it every 4 h. In early time points, Baf A1 treatment has not effect over cell viability **(Figures 1 & 2)**, even at high concentrations **(Figure 2)**. After 24 h, we observed a strong effect of Baf A1 treatment over cellular morphology, phenomenon stronger in OKO cells **(Figure 1A)**. We quantified the proportion of death cells in each time point, normalizing the number of positive YOYO-1 cells versus sir-DNA positive cells. Cell viability started to be affected just after 16h, starting from 5 nM **(Figure 1B)**, and similar at higher Baf A1 concentrations **(Figure 2)**. Surprisingly, in all the tested concentrations, OKO cells are more susceptible to the inhibition of lysosomal acidification, indicating that OMA1 plays a pro-survival role in these conditions.

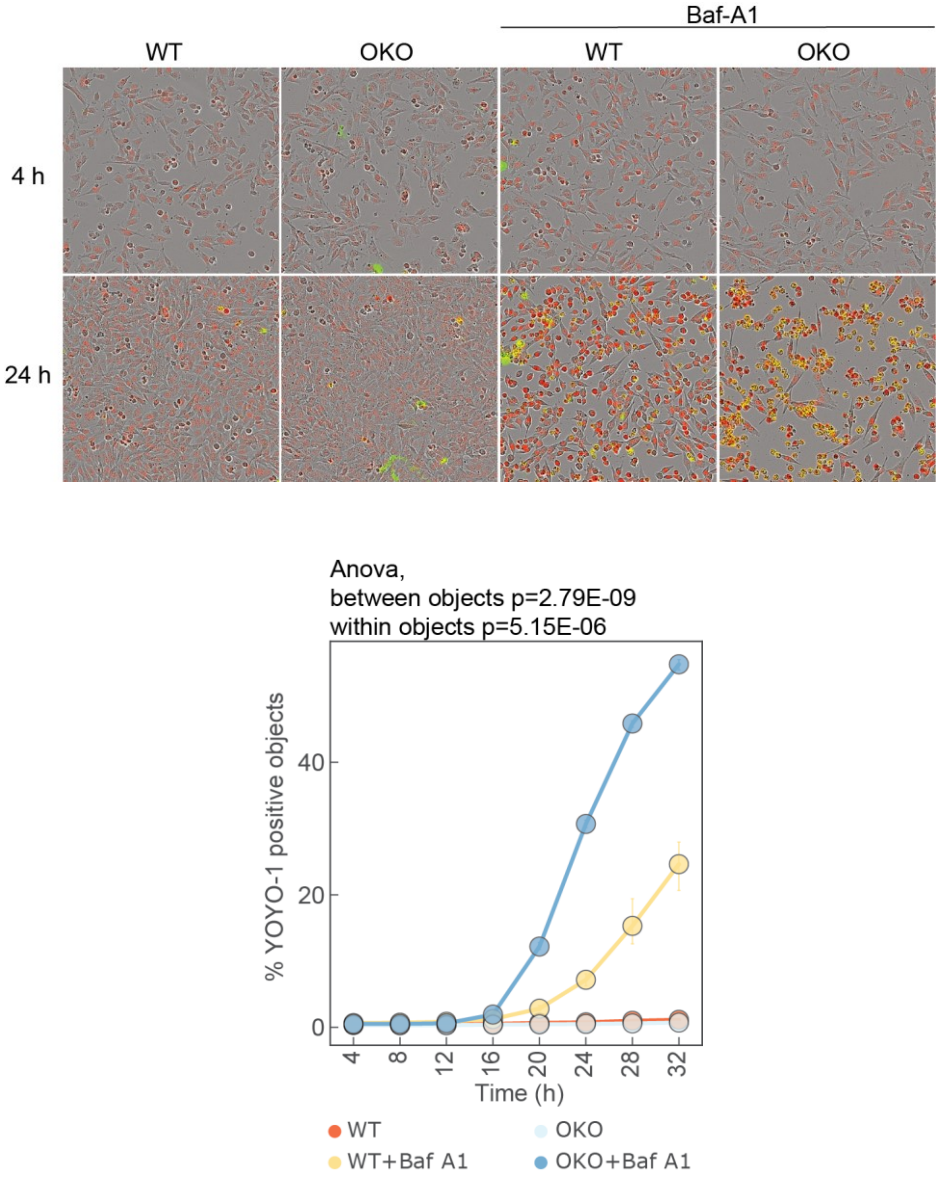

Figure 1. Baf A1 treatment affects cell viability and OMA1 protects against cell death.

A) Representative images at 4 and 24 h of WT and OKO MEF cells treated with Baf A1 (5 nM) and stained with sir-DNA (red), a cell permeable nucleic-acid dye used to quantify total cell number and YOYO-1 (green), a cell impermeable nucleic-acid dye used to quantify cells that are undergoing cell death. B) Cell death kinetic of WT and OKO MEF cells treated with Baf A1 (5 nM). Pictures were captured every 4 h per 32 h. Percentage of YOYO-1 positive objects represent the amount YOYO-1 positive cells (death cells), normalized to the total cell number (sir-DNA positive objects) .n=3, two-way ANOVA with one repeated measure. Data are shown as mean± 95% CI.

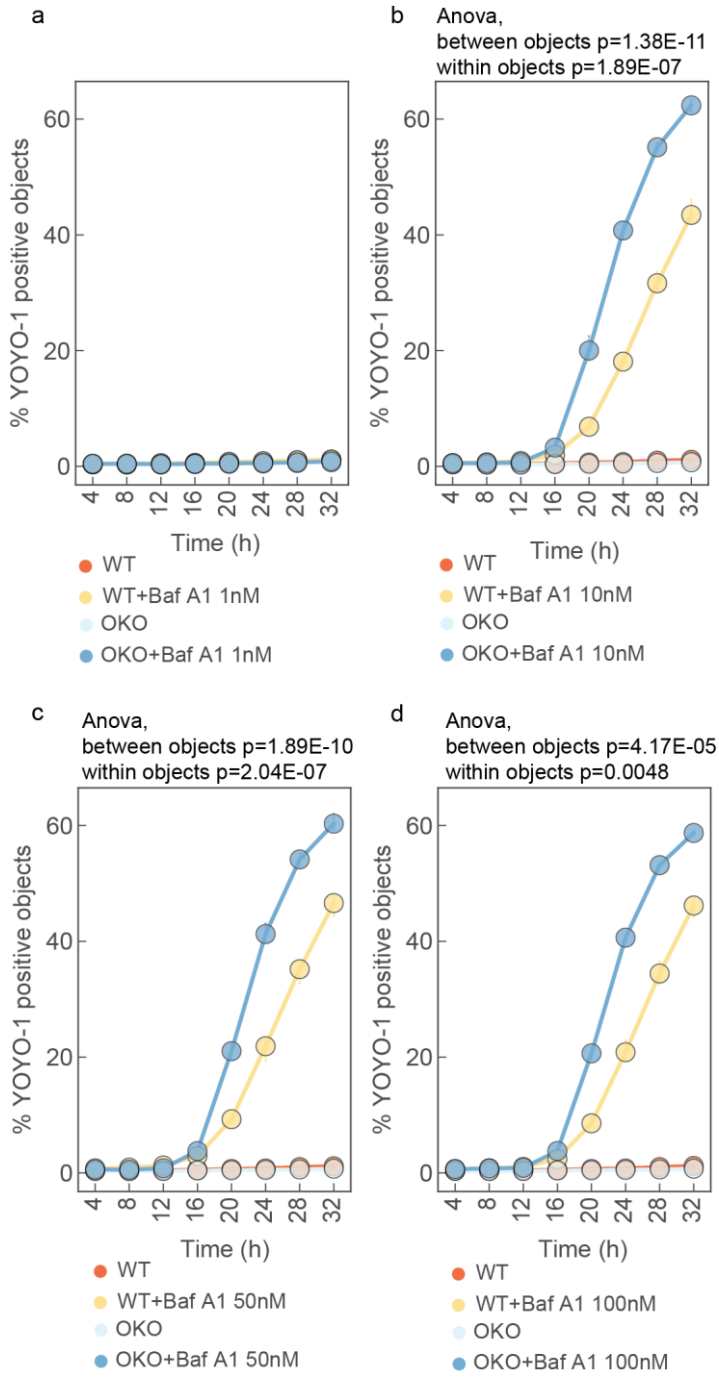

Figure 2. Loss of lysosomal acidification induces cell death in late time points independently of the concentration.
Cell death kinetics of WT and OKO MEF cells treated with Baf A1. **a)** 1 nM, **b)** 10nM, **c)** 50 nM and **d)** 100 nM. Pictures were captured every 4 h per 32 h. Percentage of YOYO-1 positive objects represent the amount of cells with plasma membrane permeabilization (YOYO-1 positive objects) normalized to the total cell number (sir-DNA positive objects) .n=3, two-way ANOVA with one repeated measure. Data are shown as mean ± 95%CI.

To find out which type of cell death is induced by the loss of lysosomal acidification, we checked cell death in cells incubated with the pan-caspase inhibitor Z-VAD-FMK, in presence or absence of Baf A1 (5 nM), the minimal concentration tested that can induce cell death. Z-VAD-FMK reduces cell death induced by loss of lysosomal acidification in OKO cells **(Figure 3)**, showing that the decrease in cell viability in these cells is dependent of caspase activation. Nevertheless, inhibition of caspases does not fully rescue cell death in WT and OKO cells, indicating the contribution of a different cell death pathway **(Figure 3)**.

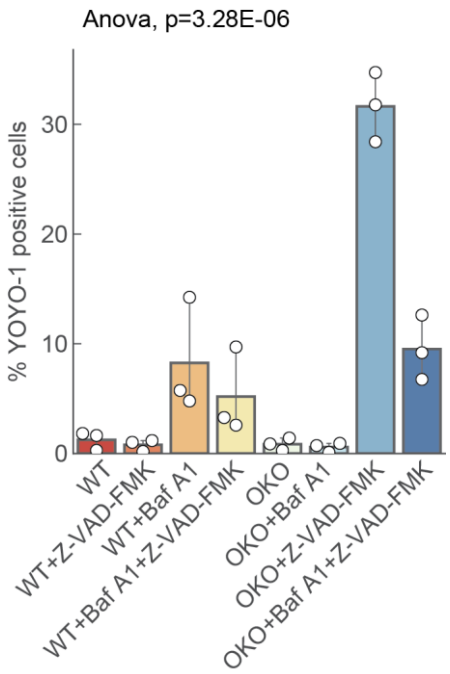

Figure 3. OMA1 prevents caspase dependent cell death induced by decrease of lysosomal acidification.
Quantification of cell death in WT and OKO MEF cells treated with Baf A1 (5 nM) in absence or presence of the pan-Caspase inhibitor Z-VAD-FMK (30 μM) for 24 h. Percentage of YOYO-1 positive objects represent the amount of cells with plasma membrane permeabilization (YOYO-1 positive objects) normalized to the total cell number (sir-DNA positive objects). n=3, two-way ANOVA, Data are shown as mean ± 95%CI.

To support our data of caspase dependent cell death, we performed fluorescent-activated cell sorting (FACS) experiments to analyse different population of death cells under Baf A1 treatment. We labelled the cells with NucView, a cell permeable dye that emits fluorescence under the activation of Caspase3/7, and RedDot2, a cell impermeable nucleic acid dye. Loss of lysosomal acidification reduced in 50% the cell viability of OKO cells, corresponding to the double negative cells **(Figure 4A)**. 30% of OKO cells treated with Baf A1 are positive for late apoptosis, a similar value obtained with YOYO-1 experiments **(Figure 4B)**. The rest 20% of death cells are positive for "early" apoptosis. We did not observed any population of necrotic cells neither in WT nor in OKO cells **(Figure 4B)**.

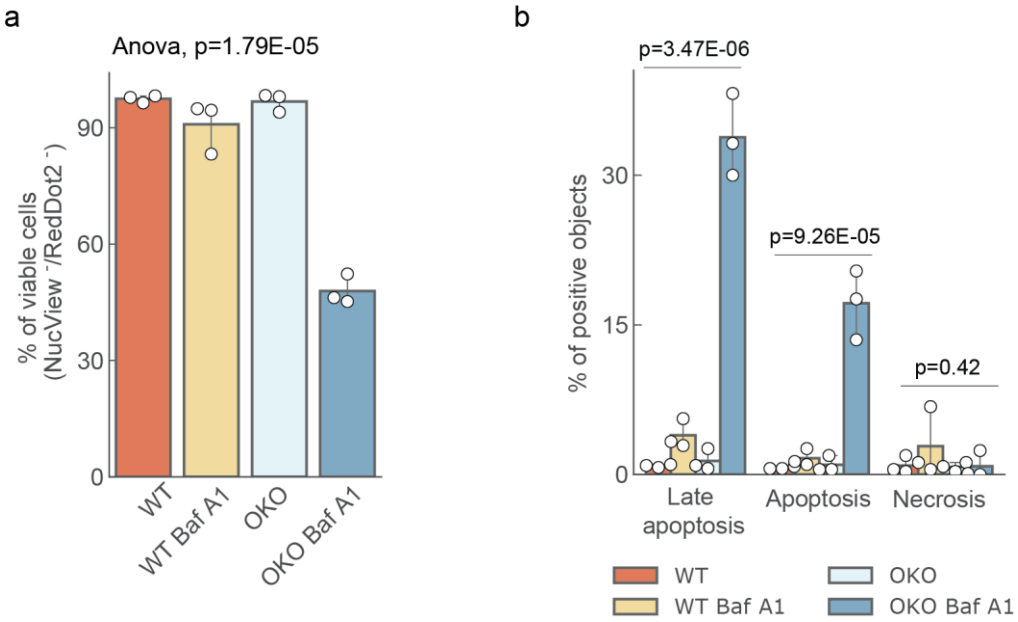

Figure 4. OMA1 prevents apoptotic cell death induced by loss of lysosomal acidification.
Quantification of cell populations stained with RedDot (plasma membrane permeabilization) and NucView (Caspase 3/7 activation). **A)** Viable cells = Nucview negative, RedDot negative cells. **B)** Apoptotic cells = NucView positive, RedDot negative cells; Late apoptotic cells = NucView positive, RedDot positive cells; Necrotic cells = NucView negative, RedDot positive cells. n=3, two way ANOVA. Data are shown as mean ± 95%CI.

Finally, to comfirm the activation of the apoptotic pathway, we checked the cleaved forms of Caspase-3 and PARP, indicators of the apoptotic pathway activation **(66, 67)**. Loss of lysosomal acidification increases the levels of cleaved PARP (c-PARP) and cleaved Caspase-3 (c-Casp3) in OKO cells **(Figure 5)**, confirming the activation of this pathway showed with YOYO-1 and FACS experiments. All together, these data shows that the loss of lysosomal acidification impears cell viability, and that the mitochondrial protease OMA1 is necessary to prevent apoptosis, and no other type of cell death.

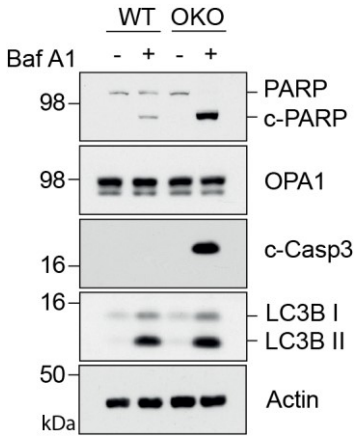

Figure 5. OMA1 prevents activation of the caspase pathway under loss of lysosomal acidification.
Representative Western blot of cell lysates from WT and OKO MEF cells treated with Baf A1 5 nM for 24h. c-PARP, cleaved form of PARP. C-Casp3, cleaved and active form of Caspase-3. n=3.

Loss lysosomal acidification impairs several functions of this organelle, including the degradation process of cellular material called autophagy **(68)**. Autophagy plays an important role in mitochondrial quality control, degrading dysfunctional and possibly harmful mitochondria, process known as mitophagy. During mitophagy, dysfunctional mitochondria can be engulfed by an autophagosomal membrane, being finally delivered into lysosomes where is finally degraded by acidic proteases **(69)**. Autophagy can be also a source

of nutrients for mitochondria under starvation **(70)**. Considering this, we wonder if the effect of Baf a1 treatment is due to the block of the autophagy-lysosomal pathway. First, we decided to target the early steps of autophagy by using esiRNA against ULK1 or BECN1, two proteins that play a central role in autophagy initiation **(71)**. Neither ULK1 *knock down* (KD) nor BECN1 KD activates the apoptotic pathway in WT or OKO cells **(Figure 6)**.

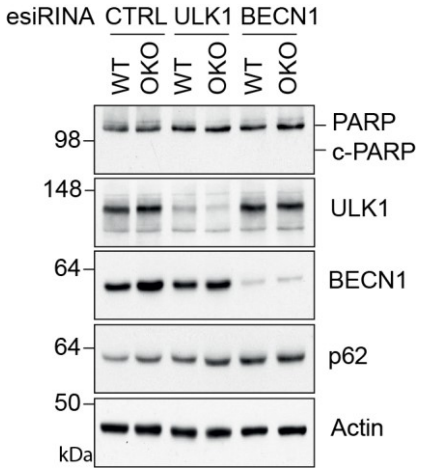

Figure 6. Autophagy inhibition does not induce cell death in neither WT nor OKO cells.
Representative Western blot of cell lysates from WT and OKO MEF cells transfected with esiRNA for ULK1 or BECN1 by 72 h. c-PARP, cleaved form of PARP. c-Casp3, cleaved and active form of Caspase-3.n=3.

Lysosomes are also the end stage of other types of autophagic degradation, like chaperone-mediated autophagy and microautophagy **(72)**. To discard the role of any of these pathways in the cell death induced by loss of lysosomal acidification, we cultured cells with E-64, an inhibitor of cysteine proteases, and pepstatin A, inhibitor of acidic proteases, in order to inhibit lysosomal degradation of cargos coming from different pathways **(73)**. Proteases inhibitors do not induce cell death neither in WT nor in OKO cells **(Figure 7)**, suggesting that the effect of loss of lysosomal acidification over cell viability is not related to the degradative role of lysosomes.

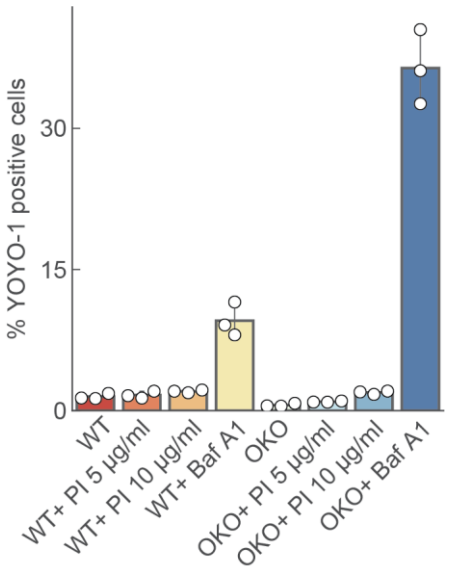

Figure 7. Lysosomal protease inhibitor does not induce cell death neither WT nor OKO cells.
Quantification of cell death in WT and OKO MEF cells treated either with Baf A1 (5 nM) or protease inhibitors (PI) for 24 h. Percentage of YOYO-1 positive objects represent the amount of cells with plasma membrane permeabilization (YOYO-1 positive objects) normalized to the total cell number (sir-DNA positive objects). n=3. Data are shown as mean ± 95% CI.

In order to support the idea that the loss of lysosomal acidification affects cell viability, we treated cells with Concanamycin A (Con A), an endo-lysosomal V-ATPase inhibitor with high selectivity **(74)**. Con A treatment activates apoptosis in WT and OKO cells, but with stronger effects over cells lacking OMA1 **(Figure 8)**.

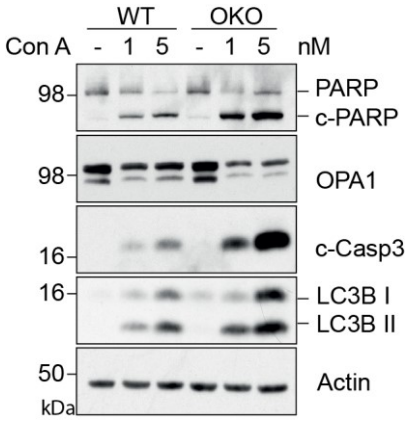

Figure 8. OMA1 prevents apoptosis activation induced by loss of lysosomal acidification.
Representative immunoblot of cell lysates from WT and OKO MEF cells treated with Concanamycin-A (Con A) 1 and 5 nM for 24h. c-PARP, cleaved form of PARP. c-Casp3, cleaved and active form of Caspase-3.n=3.

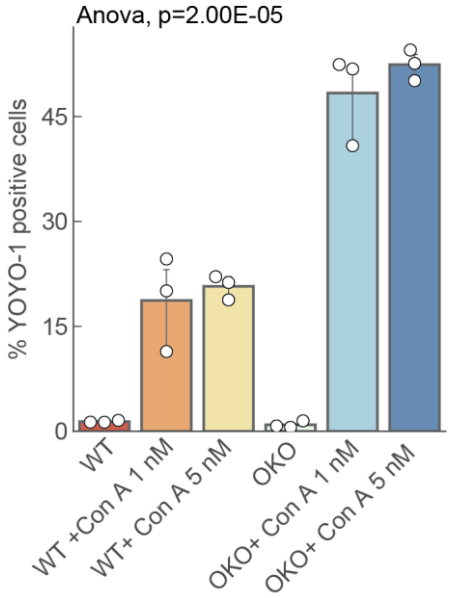

Figure 9. OMA1 protects against cell death induced by loss of lysosomal acidification.
Quantification of cell death in WT and OKO MEF cells treated with Concanamycin-A (Con A) and stained with YOYO-1 (death cells) and sir-DNA (total cell number) per 24 h. n=3, two-way ANOVA. Data are shown as mean ± 95% CI.

We confirm this result with the YOYO-1 cell death assay, showing that OKO cells are more susceptible to Con A treatment **(Figure 9)**, supporting the idea that OMA1 is necessary to prevent apoptotic cell death when the acidification of lysosomes is impaired.

OMA1 has been mostly reported as a pro-apoptotic protease in mammals, regulating the processing of the pro-fusion protein OPA1. OMA1 claves OPA1, limiting mitochondrial fusion, and later on leading to fragmentation **(17)**. Wondering if the pro-survival role of OMA1 under loss of lysosomal acidification also depends on the cleavage of OPA1, we asses immunoblotting experiments in order to verify any change in OPA1 isoforms and forms. Baf A1 treatment does not induce any changes in the levels of OPA1 long or short forms unlike CCCP treatment **(Figure 10)**, a well-known OMA1 activator **(23)**, indicating that OMA1 prevents cell death under loss of lysosomal acidification via an OPA1 independent mechanism.

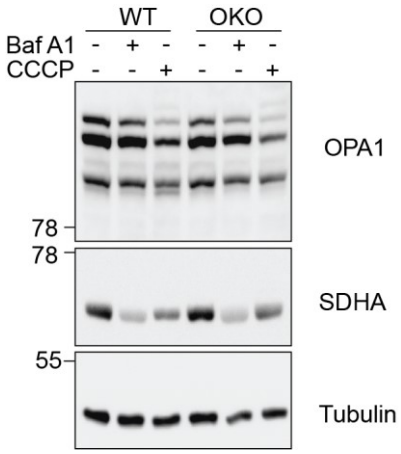

Figure 10. Loss of lysosomal acidification does not induce OPA1 processing. Representative immunoblot of cell lysates from WT and OKO MEF cells treated with Baf A1 (5 nM) for 24 h or Carbonyl cyanide 3-chlorophenylhydrazone (CCCP) 20 μM per 2 h. n=3.

In yeast cells, loss of lysosomal acidification induces mitochondrial dysfunction during replicative aging **(40)**. Something similar is observed in mammalian cells, where the pharmacological inhibition of lysosomal acidification also impairs OXPHOS **(75)**. Wondering if the same is happening in our system and if OMA1 plays any role regulating OXPHOS, we performed seahorse experiments allowing us to have a general picture of mitochondrial homeostasis under stress.

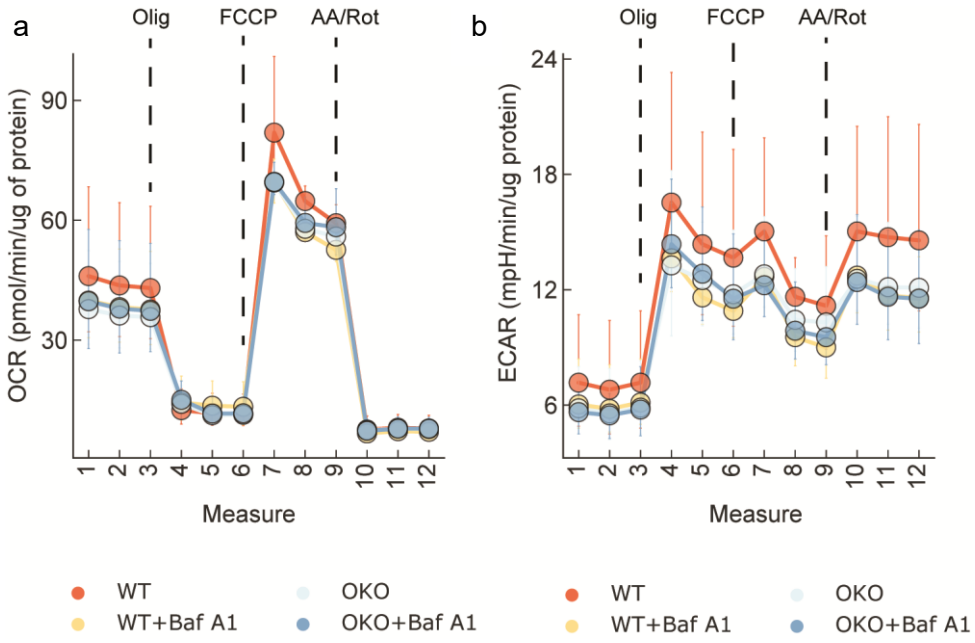

Figure 11. Loss of lysosomal acidification does not affect OCR or ECAR in early time points.
A) Oxygen consumption rate (OCR) curve of WT and OKO MEF cells treated or untreated with Baf A1 (5 nM) for 6 h. **B)** Extracellular acidification rate (ECAR) curve of WT and OKO MEF cells treated or untreated with Baf A1 (5 nM) for 6 h. Complex V inhibitor Oligomycin (Olig) 2 μM, the uncupler FCCP 0,5 μM and the complex I and complex III inhibitors Antimycin A (AA) and Rotenone (Rot) were added sequentially at the indicated points. n=3. Data are shown as mean ± 95% CI.

First, we address if there are any effect over OCR or ECAR in early time points of loss of lysosomal acidification. The treatment with Baf A1 per 6 h does not affect any OCR parameter or ECAR **(Figure 11A-B)**, suggesting that loss of lysosomal acidification does not have acute effects over mitochondrial homeostasis. Second, in order to verify the effect over respiration in late time points, we treated cells with Baf A1 per 16 h, a time point where the cell viability is yet not affected **(Figure 1B)**. The 16 h treatment decreased all OCR parameters in WT and OKO cells, showing a strong OXPHOS defect **(Figure 12A-B)**. From these results, we can conclude that the reduction of oxygen consumption induced by loss of lysosomal acidification is a long-term phenomenon where OMA1 does not play any role, indicating that the pro-survival role of OMA1 is independent of OXPHOS. Interestingly, loss of lysosomal acidification does not induce clear changes in ECAR **(Figure 13)**.

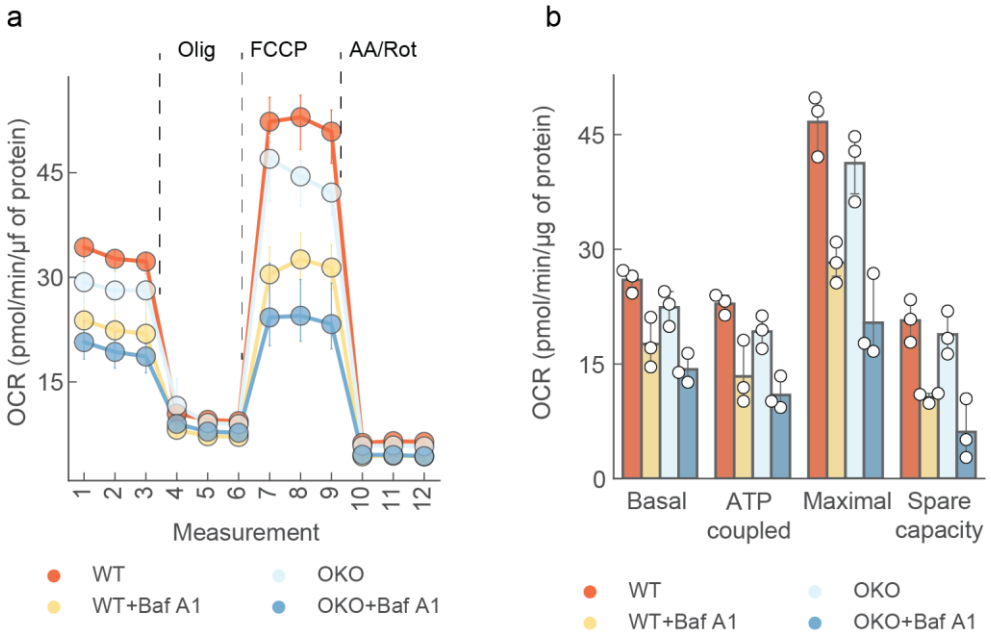

Figure 12. Loss of lysosomal acidification decrease respiration in late time points.

A) Oxygen consumption rate (OCR) curve of WT and OKO MEF cells treated or untreated with Baf A1 (5 nM) for 16 h. Complex V inhibitor Oligomycin (Olig) (2 µM), the uncoupler FCCP (0,5 µM) and the complex I and III inhibitors Antimycin A (AA) and Rotenone (Rot) were added sequentially at the indicated points. **B)** Quantification of OCR parameters from the experiment showed in A). Basal OCR is measure as the baseline respiration. ATP coupled is the proportion of OCR that contributes to ATP synthesis (measured as the decrease of OCR upon Oligomycin treatment). Maximal OCR show the maximal OCR capacity of the mitochondria can achieve stimulated by FCCP treatment. Spare respiratory indicates the capability of the cell to respond to an energetic demand as well as how closely the cell is to respiring to its theoretical maximum. n=3. Data are shown as media ± 95% CI.

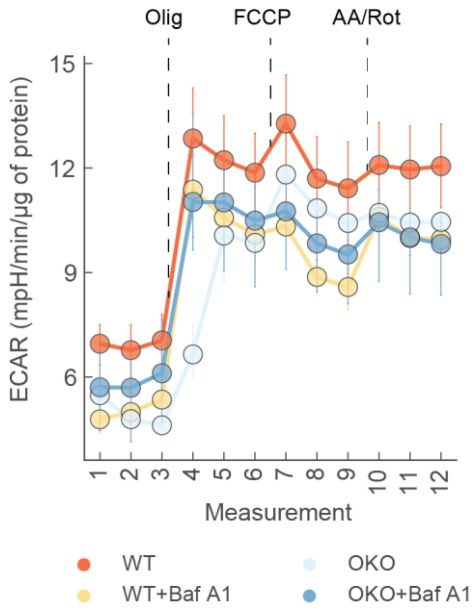

Figure 13. Loss of lysosomal acidification does not affect extracellular acidification in late time points.
Extracellular acidification (ECAR) of WT and OKO MEF cells treated with Baf A1 (5 nM) for 16 h. Complex V inhibitor Oligomycin (Olig, 2 µM), the uncoupler FCCP (0,5 µM) and the complex I and III inhibitors Antimycin A (AA) and Rotenone (Rot) were added sequentially at the indicated points. n= 3. Data are shown as mean ± 95%CI.

The exact mechanism of how lysosomal dysfunction impairs mitochondrial respiration remains elusive. In *Saccharomyces cerevisiae*, loss of vacuole acidification induces mitochondrial dysfunction via a mechanism dependent of amino acids efflux from vacuoles to cytoplasm. The overexpression of vacuolar amino acids importers rescues mitochondrial dysfunction **(40)**, suggesting that amino acids overload in the cytoplasm can be part of the mechanism of mitochondria-lysosomal communication. Nevertheless, a recent study in mammalian cells showed that V-ATPase inhibition induces accumulation of amino acids within the lysosomal lumen **(76)**, showing that there are evolutionary differences in the mechanisms related to lysosomal/vacuole amino acids homeostasis. In order to address if we can observe disturbances in cellular amino acids levels, in basal or Baf A1 treated conditions, we performed metabolomics analysis of whole cell lysates. Loss of lysosomal acidification does not induce any clear tendency to either increase or decrease amino acids levels **(Figure 14)**. In basal conditions, OKO cells has reduced

glutamine levels compared to WT, and under loss of lysosomal acidification Betaine is the most affected amino acid, showing reduced levels in cell lacking OMA1 compared to WT **(Figure 14)**.

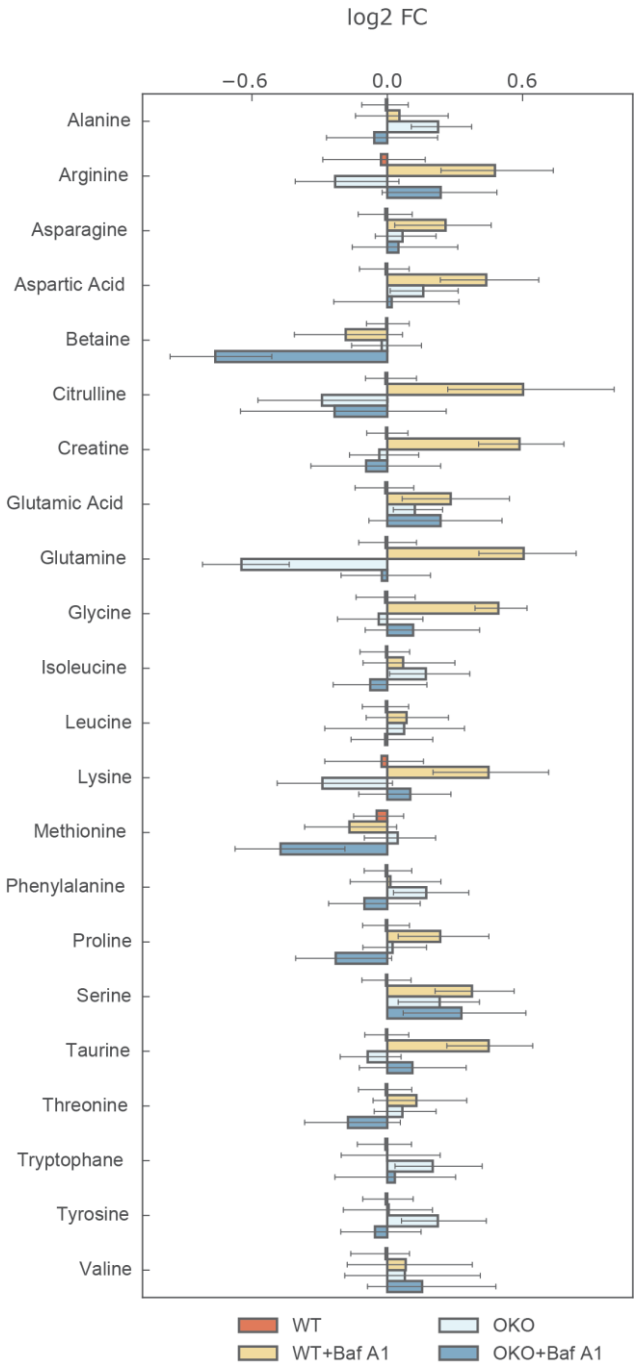

Figure 14. Effect of loss of lysosomal acidification over amino acids homeostasis.
Intracellular steady state amino-acids levels extracted from WT and OKO MEF cells cultured with Baf A1 (5 nM) for 16 h. n=5, log2 fold changes normalized to the WT untreated condition. Data are shown as mean ± 95% CI.

Glutamine is the most abundant amino acid in plasma and in the standard cell culture media. Despite being a non-essential amino acid, high concentrations of this amino acid are needed to keep cell growth in dividing cells **(77)**. Glutamine is utilized in several biosynthetic pathways, including proteins, nucleotides and glutathione synthesis **(78)**. The reduced glutamine levels in OKO cells could be due to a lower synthesis, lower uptake or to an increase in the utilization. Our cells were growth in culture media with high glutamine concentration (Glutamax ®), so even if the synthesis of glutamine is decreased, the availability of this amino acid in the media should compensate this defect and keep the steady states levels as in WT cells. In addition to glucose, glutamine is one of the main carbon sources for the TCA cycle in cell culture conditions **(79)**. The incorporation of glutamine can be assessed performing stable-isotope labelling experiments **(Figure 15)**. Briefly, cells are fed with uniformly labelled ^{13}C-glutamine (U-^{13}C-glutamine), where all the carbons of the structure are ^{13}C isotopes. Once glutamine is metabolized to glutamate and then to α-ketoglutarate, the carbons can follow an oxidative pathway, replenishing TCA cycle metabolites (Anaplerosis). Nevertheless, in conditions where OXPHOS is compromised, glutamine carbons can follow an alternative cytosolic pathway, called reductive carboxylation **(80, 81)** (**Figure 15)**. Wondering if the reduction in Glutamine steady state levels in OKO cells is due to an increase into its incorporation into TCA cycle and if loss of lysosomal acidification is inducing reductive carboxylation, we cultured cells in U-^{13}C-glutamine-containg media and treated the cells with Baf A1 per 16 h.

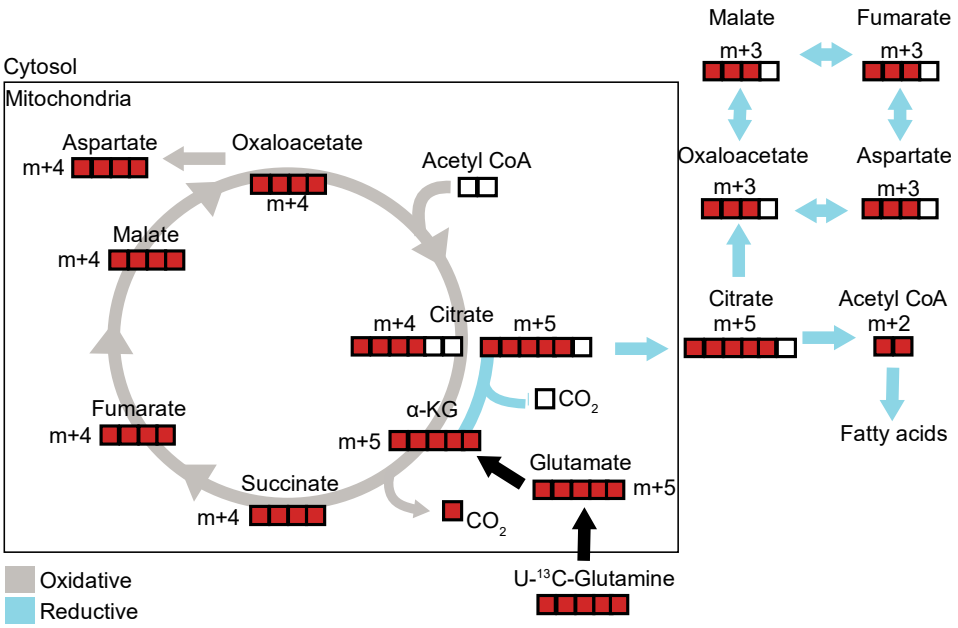

Figure 15. Scheme of glutamine oxidative and reductive metabolism measured with uniformly labelled ^{13}C-Glutamine (U-^{13}C-Glutamine).
Oxidative (anaplerotic) pathway is represented in grey. Reductive carboxylation is represented in light blue. Red and white squares represents labelled and un-labelled carbons, respectably, in the TCA cycle metabolites.

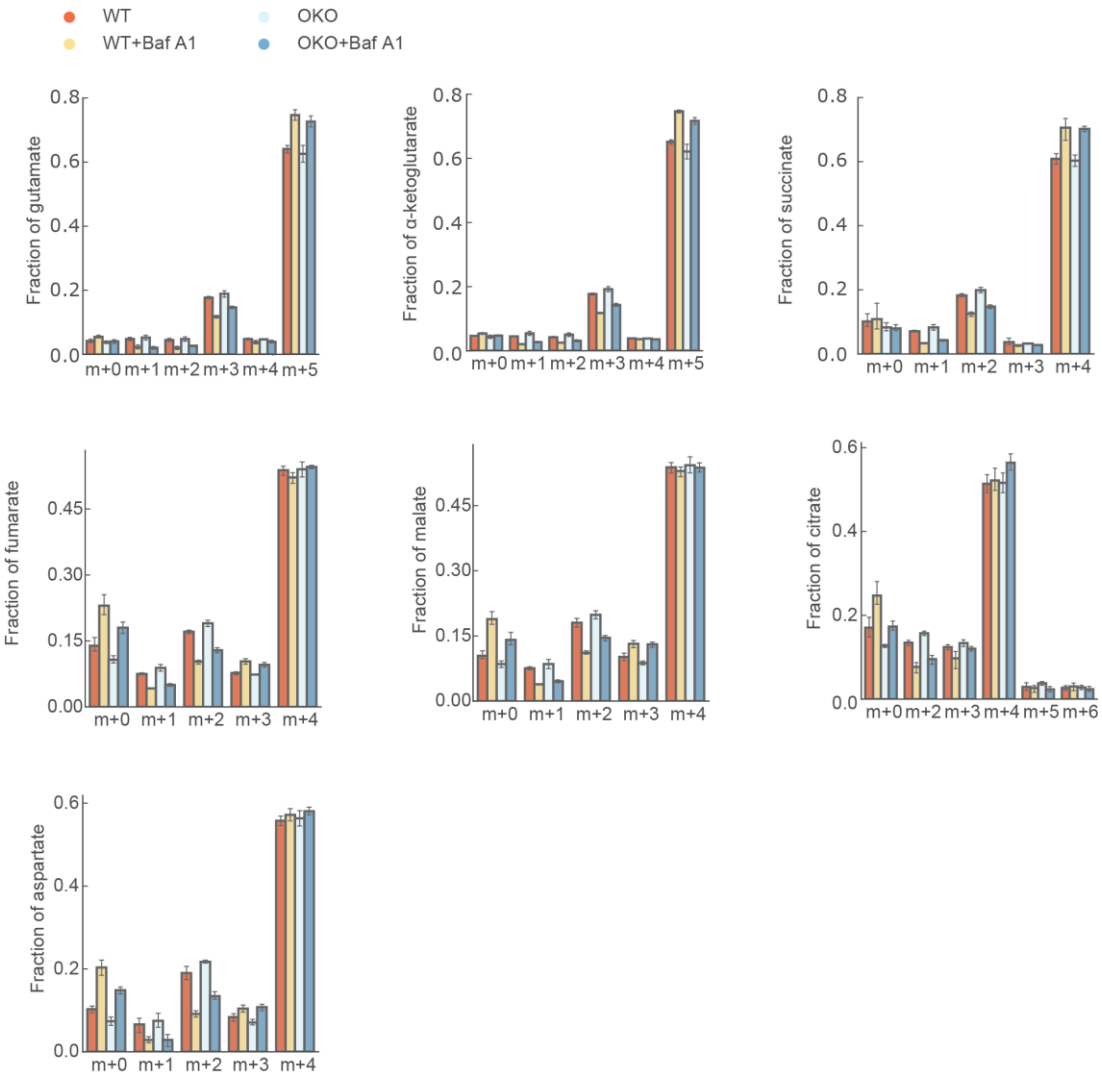

Figure 16. Fractions of glutamine incorporation into TCA metabolites.
Fractions of isotopologues from TCA cycle metabolites extracted from WT and OKO MEF cells treated with Baf A1 (5 nM) 16 h cultured with U-^{13}C-Glutamine. Fractions are obtain from the normalization of each isotopologue intensity normalized to the total sum of isotopologues intensities (m+n/ (m+0+m+1+m+n…)). n=5. Data are shown as mean ± 95% CI.

First, we analysed the fractions of each isotopologue. m+3 fractions of fumarate, malate and aspartate are indicators of an increase in reductive carboxylation. Loss of lysosomal acidification slightly increase m+3 fractions of these metabolites **(Figure 16)**, that correlates with the decrease, but not completely block of OXPHOS activity. There are no differences between OKO and WT cells, indicating that OMA1 it is not necessary to induces reductive carboxylation. Second, m+5 fractions of glutamate and α-ketoglutarate and m+4 fraction of succinate are increase under loss of lysosomal acidification. Nevertheless, m+4 fractions of fumarate, malate, aspartate and citrate are not changed. Interestingly, m+1 and m+2 fractions of all the TCA cycle metabolites analysed are decreased, indicating that the sequential cycles of glutamine into the cycle are reduced **(Figure 16)**. To address this question, we normalized the same metabolomics data against the m+0 (unlabelled) fraction, to see the general levels of glutamine incorporation. Surprisingly, m+4 fractions are strongly affected just after the step between succinate and fumarate, indicating that the loss of lysosomal acidification impairs this specific step **(Figure 17)**.

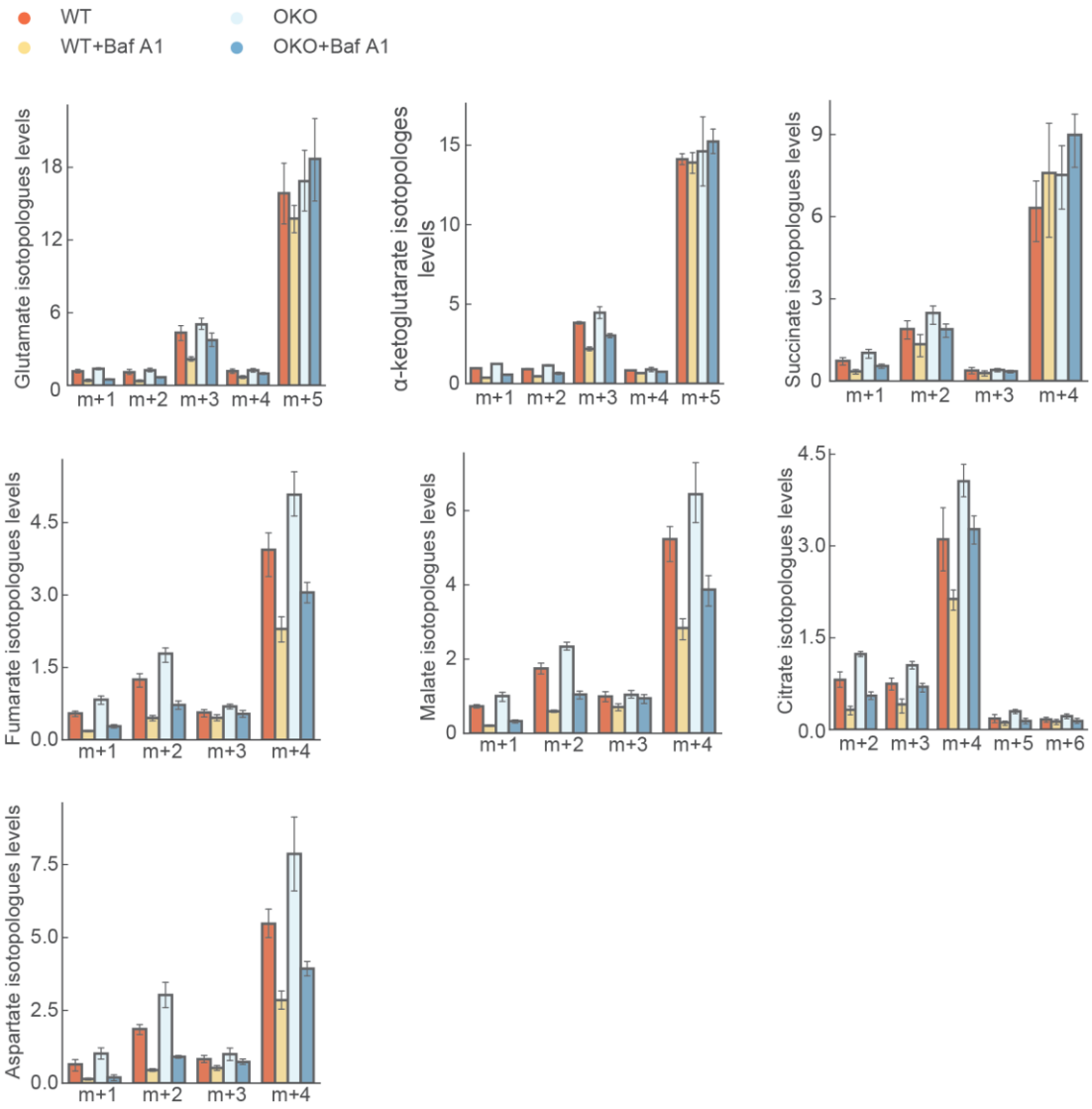

Figure 17. Glutamine incorporation into TCA cycle metabolites.
Fractions of isotopologues from TCA cycle metabolites extracted from WT and OKO MEF cells treated with Baf A1 (5 nM) for 16 h cultured with U-^{13}C-Glutamine. Isotopologues levels are obtained from the normalization of each isotopologue intensity normalized to the unlabelled fraction (m+n/m+0). n=5. Data are shown as mean ± 95% CI.

Succinate dehydrogenase (SDH) is the enzyme that metabolised succinate to fumarate and is composed by four subunits: SDHA, SDHB, SDHC and SDHD. This complex is part of both ETC and TCA cycle **(82)**. In order to analyse if the loss of lysosomal acidification affects SDH subunits, we performed immunoblot experiments to determine SDHA and SDHB protein levels. Loss of lysosomal acidification reduces SDHA and SDHB protein levels in WT and OKO cells **(Figure 18)**, result that explain the effect of Baf A1 treatment over TCA cycle metabolites.

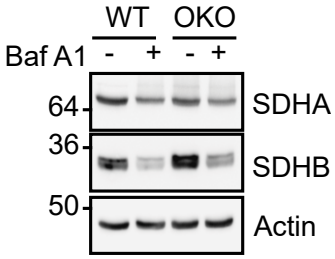

Figure 18. Loss of lysosomal acidification decrease SDHA and SDHB protein levels.
Representative immunoblot of cell lysates from WT and OKO MEF cells treated with Baf A1 (5 nM) for 16h. n=3.

Endo-lysosomes play a central role in iron uptake and homeostasis, being part of the transferrin cycle (endosomes and lysosomes) and mediating ferritin degradation (lysosomes) **(83)**. Importantly, both pathways require the acidic pH, kept by V-ATPase activity **(84)**. Supporting the role of endo-lysosomal acidification on iron homeostasis, Baf A1 treatment for 24 h results on intracellular Iron depletion leading to HIF1α stabilization, phenomenon rescued by iron supplementation **(85)**.

SDHB sub-unit is an iron-sulfur cluster containing protein, being sensitive to defects in the iron-sulfur cluster biogenesis pathway, as well as to defects on iron acquisitions, leading to SDHB destabilization **(86-88)**. Considering the strong reduction of SDHB levels under loss of lysosomal acidification, we hypothesised that Baf A1 treatment induces iron starvation, causing defects in mitochondrial respiration. First, we assess the induction of iron starvation

response under Baf A1 treatment, analysing Transferrin receptor (TfR) protein levels, a marker of iron starvation response **(83, 89)**. Loss of lysosomal acidification increases TfR protein levels as the iron chelator Deferipron (DFP) **(Figure 19)**, confirming that the inhibition of the endo-lysosomal V-ATPase leads to a decrease of iron availability, as reported previously **(85)**. Iron-sulfur cluster biogenesis, a synthetic pathway where mitochondria play a fundamental role, relays in the availability of iron **(90)**. Supporting the idea that loss of lysosomal acidification impairs iron homeostasis, Baf A1 treatment reduces the iron-sulfur cluster binding protein NDUFS1, component com the mitochondrial complex I and SDHB **(Figure 19)**, suggesting that the cause of OXPHOS dysfunction under Baf A1 treatment is due to a decrease of iron-sulfur cluster biogenesis.

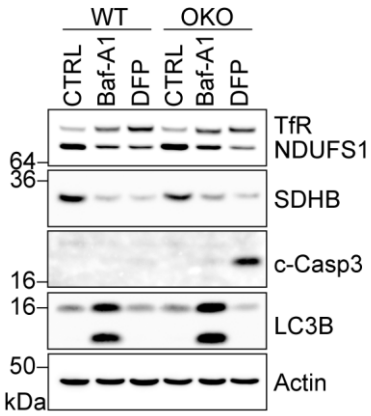

Figure 19. Loss of lysosomal acidification induces the iron starvation response. Representative immunoblot of cell lysates from WT and OKO MEF cells treated with Baf A1 (5 nM) or Deferiprone (DFP, 100 μM) for 16 h. TfR, Transferrin receptor. c-Casp3, cleaved and active form of Caspase-3. n=3.

Iron starvation induced by loss of lysosomal acidification is rescued by supplementation with iron-citrate in the cell culture media **(85)**. Taking that idea, first we address whether iron supplementation can rescue the decrease of mitochondrial respiration induced by Baf A1 treatment.

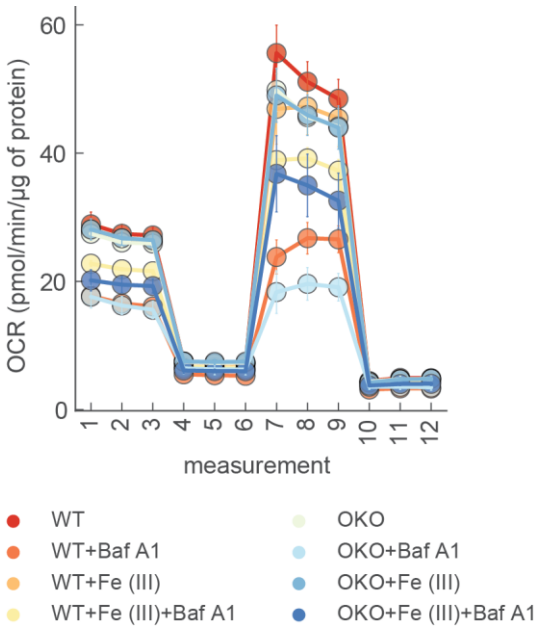

Figure 20. Iron supplementation partially rescues respiration.
Oxygen consumption rate (OCR) curve of WT and OKO MEF cells treated or untreated with Baf A1 (5 nM) for 16 h and cultured with Iron Citrate (Fe(III)) 50 µM. Complex V inhibitor Oligomycin (Olig, 2 µM), the uncoupler FCCP (0,5 µM) and the complex I and III inhibitors Antimycin A (AA) and Rotenone (Rot) were added sequentially at the indicated points. n=3. Data are shown as mean ± 95% CI.

Iron supplementation partially rescues the decrease of mitochondrial respiration in WT and OKO cells treated with Baf a1 **(Figures 20 & 21)**. Then, we checked the levels of iron-sulfur cluster binding proteins in cells cultured with iron-citrate. Interestingly, iron supplementation fully rescues NDUFS1 and SDHB protein levels under loss of lysosomal acidification **(Figure 22)**, indicating that the loss of these proteins is due to defects in general cellular iron homeostasis.

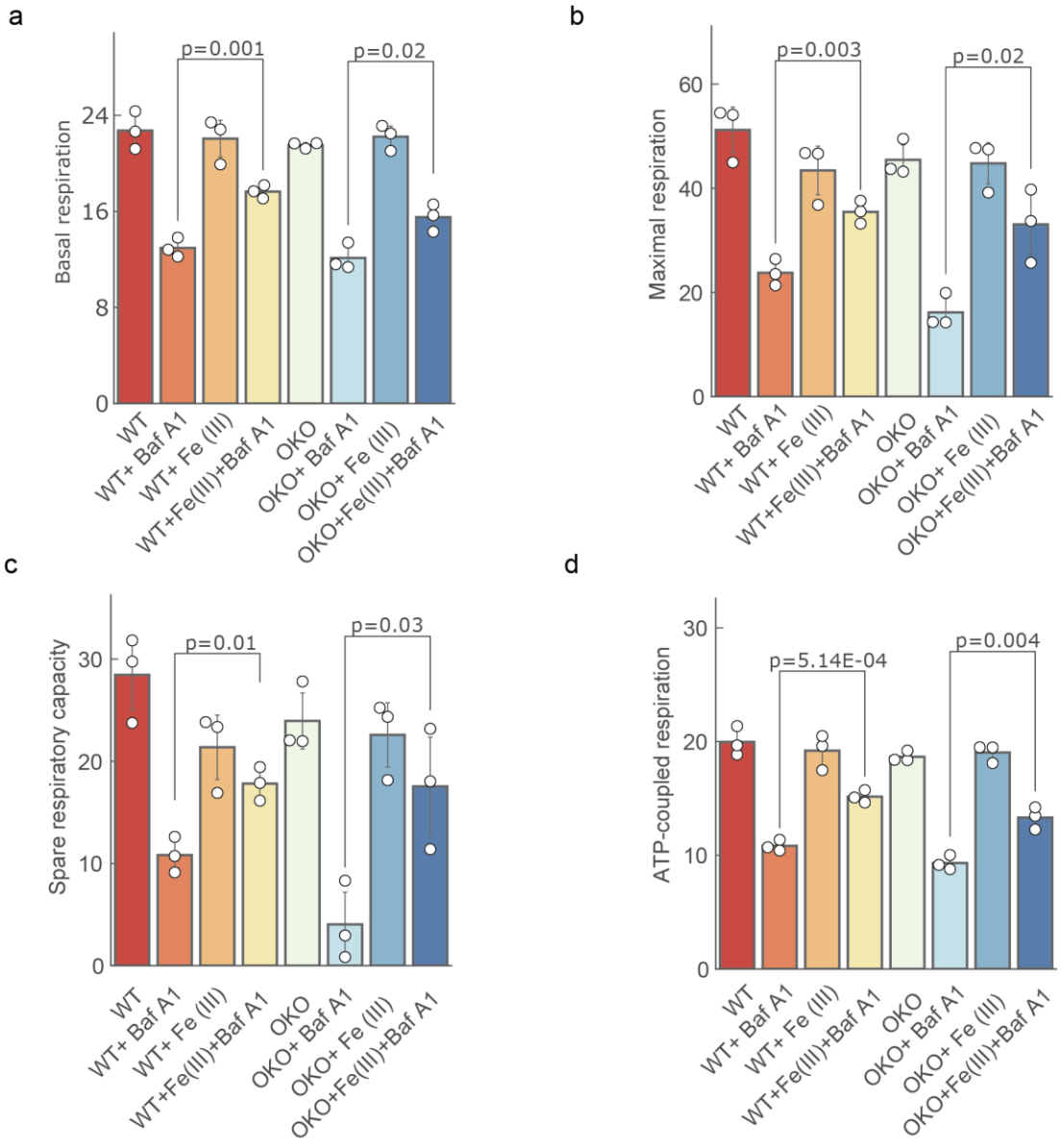

Figure 21. Iron supplementation partially rescues OCR parameters.
Quantification of OCR parameters from the experiment showed in Figure 21. **A)** Basal OCR is measure as the baseline respiration. **B)** Maximal OCR show the maximal OCR capacity of the mitochondria can achieve stimulated by FCCP treatment. **C)** Spare respiratory indicates the capability of the cell to respond to an energetic demand as well as how closely the cell is to respiring to its theoretical maximum **D)** ATP coupled respiration is the proportion of OCR that contributes to ATP synthesis (measure as the decrease of OCR upon Oligomycin treatment).. n=3, student t-test. Data are shown as mean ± 95% CI.

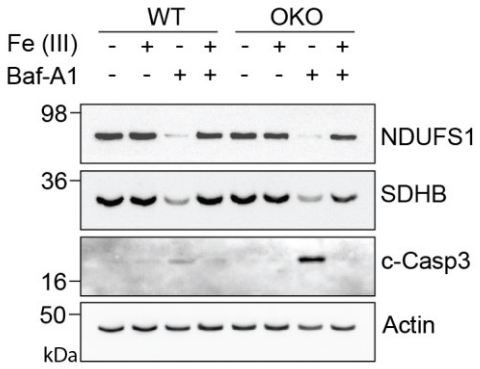

Figure 22. Iron supplementation rescues iron-sulfur cluster binding protein levels and Caspase-3 activation.
Representative immunoblot of cell lysates from WT and OKO MEF cells treated with Baf A1 (5 nM) and cultured with iron citrate (Fe(III)) 50 μM for 16 h. c-Casp3, cleaved and active form of Caspase-3. n=3

Finally, we address if the restoration of iron availability can rescue the cell death phenotype in WT and OKO cells induced by Baf A1. Consistent with the rescue of iron-sulfur cluster binding proteins and mitochondrial respiration, iron supplementation fully rescues cell death in WT and OKO cells, supporting the idea that lysosomal dysfunction can induce mitochondrial dysfunction due to a decrease in iron availability. Altogether, this data shows that iron mediates the communication between mitochondria and lysosomes.

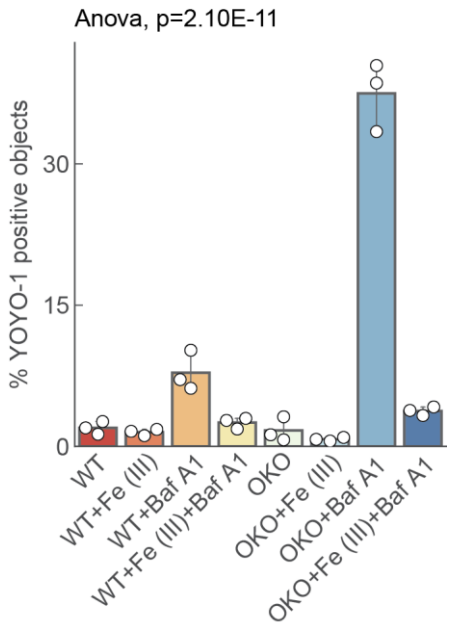

Figure 23. Iron supplementation rescues cell death induced by loss of lysosomal acidification.
Quantification of cell death in WT and OKO MEF cells treated with Baf A1 (5 nM) and cultured with iron citrate (Fe(III)) 50 µM for 24 h. Percentage of YOYO-1 positive objects represent the amount of cells with plasma membrane permeabilization (YOYO-1 positive objects) normalized to the total cell number (sir-DNA positive objects). n=3, two-way ANOVA. Data are shown as mean ± 95% CI.

Chapter II

We previously reported that mitochondrial fragmentation and loss of mitochondrial-ER contacts are two features of pathological cardiomyocyte hypertrophy **(58, 59)**. Ang-(1-9) treatment protects against ischemia/reperfusion injury *in-vivo* and *in-vitro* **(91, 92)**, and development of cardiomyocyte hypertrophy in *in-vitro* and *in-vivo* **(62, 63)**. Nevertheless, the molecular mechanism of Ang-(1-9) is not fully understood. Thinking in the tight relationship between cardiomyocyte homeostasis and mitochondria, we wonder if the mechanism of Ang-(1-9) over hypertrophy is due to the regulation of mitochondrial dynamics or mitochondria-ER communication. First, we assess the correlation between hypertrophy and mitochondrial morphology, using NE treatment as an *in-vitro* model of pathological hypertrophy. NE increases cardiomyocytes perimeter, indicating the induction of hypertrophy, and decreases mitochondrial area, indicating mitochondrial fragmentation **(Figure 24)**. Ang-(1-9) treatment prevents both phenomena, showing a correlation between the anti-hypertrophic effect of Ang-(1-9) and the regulation of mitochondrial dynamics.

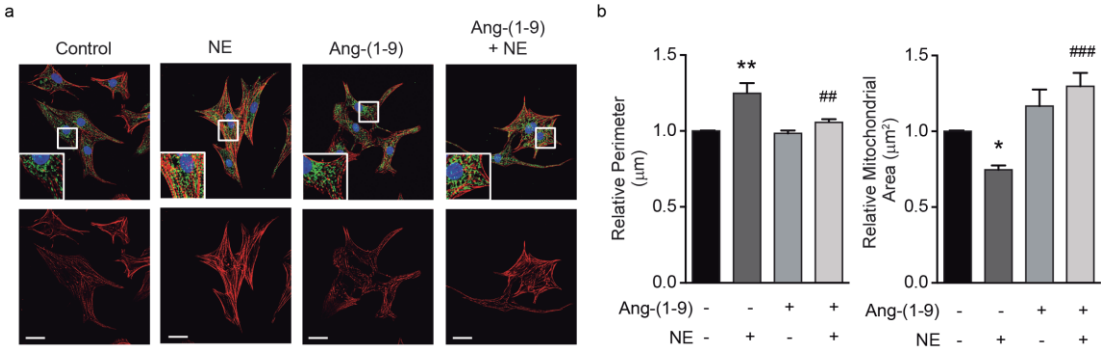

Figure 24. Angiotensin-(1-9) treatment prevents cardiomyocyte hypertrophy induced by NE.
A) Representative confocal images of cardiomyocytes treated with 100 µM Ang-(1-9) for 6 h and then stimulated with 10 µM of norepinephrine (NE) for 24 h. Cardiomyocytes were stained with rhodamine phalloidin to detect sarcomeric structures and immunolabeled for the mtHsp70 protein to identify the mitochondrial network. Scale bar: 25 µm. **B)** Quantitative analysis of relative cellular perimeter and mitochondrial area of cardiomyocytes. n=4, Data are shown as mean ± SEM. **p<0.01 vs. untreated, ##p<0.01 vs. NE. **(93)**

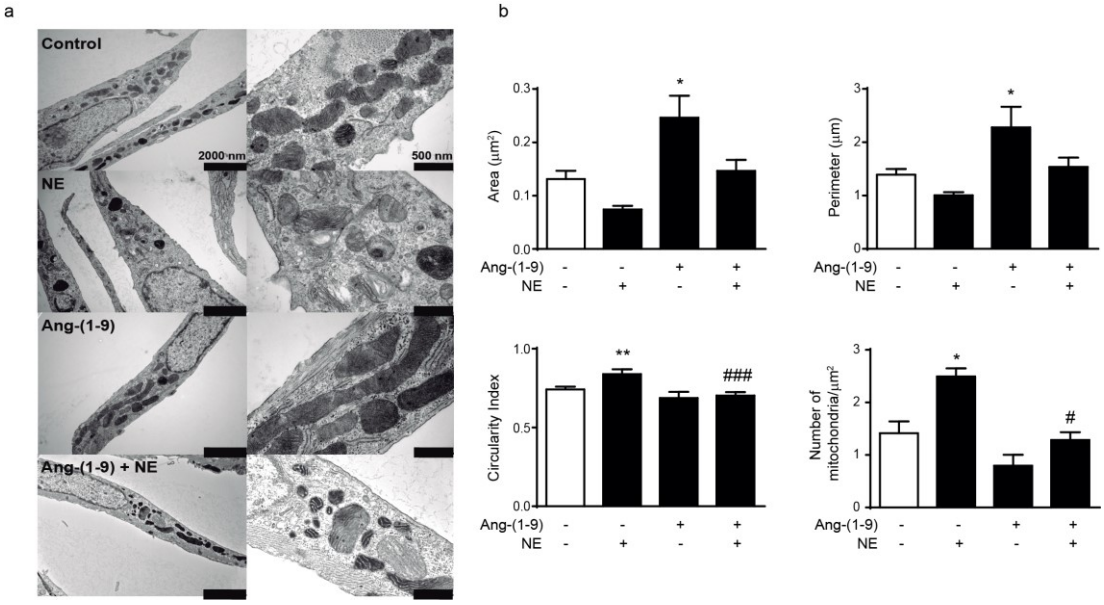

Figure 25. Angiotensin-(1-9) treatment induces mitochondrial elongation and prevents mitochondrial fragmentation induced by NE.
A) Representative transmission electron microscopy images from angiotensin-(1-9) and/or NE-treated neonatal cardiomyocytes showing two different magnifications of the same cells. **B)** Quantification of the transmission electron microscopy images shown in A). Mitochondrial area, mitochondrial perimeter, mitochondrial circularity index and number of mitochondria per area unit were obtain from 100 mitochondria of each condition, from three separate experiments. *p<0.05 and **p<0.01 vs. control; #p<0.05 and ###p<0.001 vs. NE. **(93)**

In order to confirm the effect of NE and Ang-(1-9) over mitochondrial morphology, we perform electron microscopy (EM) experiments in cardiomyocytes treated with NE and/or Ang-(1-9). EM pictures show clearly that Ang-(1-9) *per se* induces mitochondrial elongation as observed by the presence of elongated and electron dense structures **(Figure 25A)**. The opposite effect was seen in cardiomyocytes treated with NE, observing smaller and less electron dense mitochondria, effect that is prevented by Ang-(1-9) treatment (**Figure 25 A-B)**.

As we described, NE treatment also induce loss of mitochondria-ER contacts, leading to defects in mitochondrial calcium handling **(58)**. In order to investigate if the effect of Ang-(1-9) over mitochondrial morphology is also be related with the regulation of calcium homeostasis, we assess mitochondrial calcium uptake experiments in basal and NE treated conditions, in presence or absence of Ang-(1-9). As we previously reported, NE treatment decrease mitochondrial calcium uptake released from ER (histamine treatment), effect that is prevented by Ang-(1-9) **(Figure 26 A-B)**. Interestingly, Ang-(1-9) treatment itself increase mitochondrial calcium uptake. This data show that Ang-(1-9) also regulates the functional coupling between mitochondria and ER.

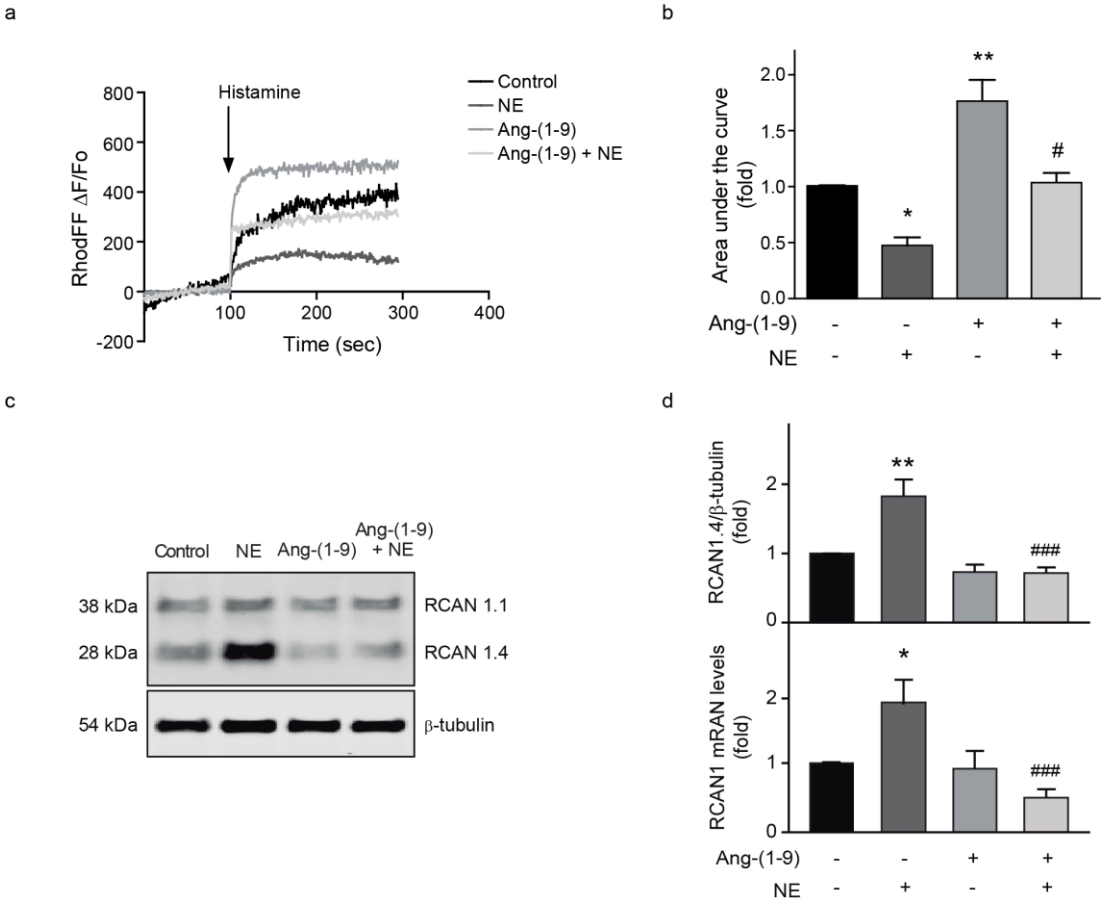

Figure 26. Angiotensin-(1-9) treatment keeps mitochondrial-ER communications and prevents the activation pro-hypertrophic signalling pathway.

A) Mitochondrial calcium kinetic of neonatal cardiomyocytes incubated with Ang-(1-9) 100 μM for 6 h and then co-cultured with NE (norepinephrine) for 24 h. Rhod-FF fluorescence was recorded with confocal microscopy using histamine (100 mM) to trigger Ca^{2+} release from the endoplasmic reticulum. **B)** Area under the curve from the kinetic showed in A) normalized to the untreated condition. **C)** Representative immunoblot from cardiomyocytes treated with Ang-(1-9) and/or NE, showing RCAN 1 isoforms. Quantification of RCAN1.4 protein and mRNA levels (n=4). *p<0.05; **p<0.01 and ***p<0.001 vs. control; $^{\#\#}$p<0.01 and $^{\#\#\#}$p<0.001 vs. NE. **(93)**

Finally, we study what it could be the connection between the regulation of mitochondrial morphology, mitochondria-ER communication and pro-hypertrophic signalling. Previous data from our group and others showed that NE treatment increases cytosolic calcium levels and activates the pro-hypertrophic signalling pathway Calcineurin/NFAT **(59, 94)**. Wondering if Ang-(1-9) treatment prevents the activation of the Calcineurin/NFAT pathway under NE treatment, we assess protein and gene expression of RCAN1.4, a downstream target of Calcineutin/NFAT **(95)**. As we previously reported, NE treatment increased RCAN 1.4 expression. Ang-(1-9) treatment prevents this effect both at protein and mRNA levels **(Figure 26C-D)**. Altogether, these data show that Ang-(1-9) treatment prevents cardiomycyte hypotrophy by keeping mitochondrial elongation and mitochondrial-ER communication, then preventing the increase of cytosolic calcium pro-hypertrophic signalling.

DISCUSSION

Chapter I

Here we described the key role of mitochondrial inter-organelle communication for cellular and organelle homeostasis. Loss of lysosomal acidification impairs mitochondrial function due to a decrease of iron availability, ion essential for iron-sulfur clusters and heme biosynthesis. On the other hand, loss of mitochondria-ER communication is related to the development of cardiomyocyte hypertrophy, and Ang-(1-9) prevents this phenomenon by regulation of mitochondrial dynamics and cytosolic calcium signalling.

The notion about lysosomal function in mammalian cells has been changing in the recent years. Lysosomes are traditionally called the “trash cans” of the cell, because several hydrolases in the lumen of this organelle degrades the cargos coming from endosomal and autophagic pathways **(96, 97)**. The activity of these hydrolases depends on the acidification of the lysosomal lumen, maintained by the V-ATPase **(98)**. Thus, V-ATPase inhibition impairs cargo degradation, leading to the accumulation of damaged proteins and/or organelles and to the reduction of recycled macromolecules (necessary under starvation conditions), affecting cell viability **(99)**. Our results showed that Baf A1 or Con A (both V-ATPase inhibitors) treatment induces cell death. Nevertheless, neither autophagy nor proteases inhibition affects cell viability, indicating that lysosomal dysfunction decrease viability independently of lysosomal proteases. However, this is true in our *in-vitro* acute V-ATPase inhibition model, thus we cannot discard the contribution of lysosomal proteolysis in chronic models of lysosomal dysfunction, as in patients and mouse models of lysosomal storage diseases **(41)**.

Besides its proteolytic function, the vision about lysosomes as central metabolic hubs has been expanded in the recent years. Membranes of yeast vacuoles (lysosomes in mammals) hold several transporters that allow the

bidirectional transport of metabolites and ions. This characteristic allows this organelle to be a reservoir of different solutes, playing an important role in metabolic homeostasis **(100)**. Several of these carriers are conserved in mammalian lysosomes, highlighting the possibility that lysosomes could play a similar role **(98)**. Supporting this hypothesis, a recent report showed that V-ATPase inhibition by Baf A1 or Con A induces the accumulation of amino acids in the lysosomal lumen after 1 h treatment **(76)**. In our work, we hypothesized those long-term treatments can lead to a cytosolic amino acid depletion, due to their retention into lysosomes. Nevertheless, we performed all our experiments with DMEM media that contains several amino acids, supplemented with non-essential amino acids, sodium pyruvate and non-dialyzed FBS. Hence, these rich-nutrient conditions make unfeasible the idea of cytosolic amino acids depletion. Supporting this, metabolomics data showed that most of the measured amino acids were unchanged in WT and OKO cells, under basal or Baf A1 treated conditions. We found that just betaine, an amino acid that plays a role in one-carbon metabolism **(101)**, is decrease in OKO cells under Baf A1 treatment. However, other amino acids involved in one-carbon pathway (like serine and glycine) do not changed, pointing that there are specific defects in betaine synthesis or utilization. Further experiments are required to determine whether betaine synthesis or utilization is affected under loss of lysosomal acidification in OKO cells.

Glutamine is the most abundant amino acid both in human bloodstream and in standard tissue culture media. Despite being a non-essential amino acid, most of the cells in culture cannot proliferate or even survive under glutamine-free conditions. Cancer cells have even greater demands for this amino acid beyond their protein synthesis requirements, making glutamine metabolic pathway a promising target for cancer treatment **(78)**. We found that glutamine steady state levels are reduced in OKO cells. Moreover, trace experiments showed that loss of OMA1 increased glutamine incorporation into the TCA cycle. In cancer cells, glutamine anaplerosis is necessary to replenish TCA cycle intermediates due to that glucose is metabolized towards lactate (aerobic

glycolysis) to generate ATP **(79)**. Lactate produced by glycolysis is secreted to the extracellular media, increasing extracellular acidification. We did not observe changes on ECAR in OKO cells, indicating not differences in aerobic glycolysis between WT and OKO cells. Therefore, the increase in glutamine anaplerosis cannot be explained by the activation of this pathway. The pyruvate generated via the glycolytic pathway is transported into the mitochondria through the mitochondrial pyruvate carrier (MPC) **(102)**. MPC inhibition or deletion in cancer or C2C12 cells increases glutamine anaplerosis, without affecting lactate secretion or OCR **(103, 104)**, a phenotype similar founded in OKO cells. The regulation of glutamine and/or glucose metabolism by OMA1 will be address in future experiments. Altogether, our data indicates that glutamine or amino acid metabolism does not play a central role in lysosomal-mitochondrial communication.

As we described, endo-lysosomal compartments play a central role in iron homeostasis. Our data shows that loss of lysosomal acidification impairs mitochondrial respiration, glutamine oxidative metabolism and the levels of the iron-sulfur cluster binding proteins NDUFS1and SDHB. Iron-sulfur cluster synthesis start within mitochondrial matrix, where after several sequential steps, iron-sulfur cluster can be incorporated into mitochondrial proteins, including ETC proteins, or be exported to the cytosol in order to synthetize cytosolic and nuclear iron-sulfur cluster binding proteins **(90)**. Iron-sulfur cluster machinery utilized ferrous iron. Iron is initially uptake from the extracellular media in its ferric form, and later on reduced within the endo-lysosomal compartments by pH dependent reductases **(84)**. Thus, V-ATPase inhibition decrease ferrous iron availability that could blunt iron-sulfur cluster synthesis and therefore decrease iron-sulfur cluster binding proteins, affecting mitochondrial respiration and TCA cycle. Our experimental data fits with this hypothesis, indicating that iron is the major contributor of lysosomal-mitochondrial communication. The rescue of respiration, iron-sulfur cluster binding proteins and cell death by iron supplementation also supports this hypothesis. Recently, several reports in yeast and mammalian cells confirm

this idea **(105-107)**. Importantly, all these phenomena are independent of OMA1 activity.

As we described, the V-ATPase is present in both endosomes and lysosomal compartments. Interestingly, a study in erythroid cells showed that iron can be directly transferred from endosomes to mitochondria, via a process called kiss-and-run **(108)**. Additionally, endosomes-containing transferrin can interact physically with mitochondria **(109)**. This rise the question if the phenotype showed in our experiments is due to an endosomal or lysosomal effect. The inhibition of lysosomal proteases does not affect cell viability, indicating that ferritin degradation within lysosomes does not play a role by itself over cell death induced by loss of lysosomal acidification. However, with our experimental approach is not possible discard neither lysosomes nor endosomes from the effect of V-ATPase inhibition.

Chapter II

Mitochondria-ER communication is an important factor in the pathophysiology of cardiovascular diseases **(110)**. NE treatment reduced mitochondria-ER colocalization, associated with a decrease of mitochondrial calcium buffering capacity **(58)**. Interestingly, our data shows that Ang-(1-9) treatment preserves mitochondrial calcium uptake capacity under NE treatment, supporting the idea that loss of mitochondrial-ER communication is a necessary step for pathological hypertrophic growth. Additionally, Ang-(1-9) treatment also preserves mitochondrial-ER colocalization under NE treatment **(93)**.
Interestingly, Ang-(1-9) treatment increases mitochondrial capacity for calcium uptake. Nevertheless, this cannot be explained by an increase of contacts between mitochondria and ER, because this treatment does no change the colocalization between these two organelles **(93)**. Ang-(1-9) treatment induces mitochondrial elongation, seeing by confocal and electron microscopy. Elongated mitochondrial network has higher calcium buffer capacity **(111,**

112), suggesting that the effect of Ang-(1-9) treatment over calcium could be explained, at least in part, by its effect over mitochondrial morphology.

This rise the question of which one is the primary effect of Ang-(1-9) that explain its anti-hypertrophic effect. Increase of cytosolic calcium levels leads to the activation of the pro-hypertrophic signalling cascade Calcineurin/NFAT **(94, 113)**. NE treatment increase the expression of RCAN1.4, a downstream target of Calcineurin/NFAT, indicating a rise in cytosolic calcium levels. Ang-(1-9) treatment prevents this phenomenon, pointing that its anti-hypertrophic effect is at least in part, due to a regulation of cytosolic calcium signalling. All this data supports the idea that mitochondrial-ER communication plays a key role in the development of cardiomyocytes hypertrophy, indicating that the transfer of calcium between these organelles is not just important to sustain bioenergetics demands, but also for the regulation of signalling pathways.

Altogether, our data shows the key role of mitochondrial inter-organelle communication in cell homeostasis and viability. Intriguingly, both in lysosome-mitochondria as well as mitochondria-ER communication, divalent metal ions are key for sustain these interactions. Mitochondria-ER contacts sites are not just the platforms for calcium transfer, are also key for lipid transport from ER to mitochondria, process fundamental to sustain mitochondrial lipid composition. In yeast, vacuole-mitochondrial contact sites, named vCLAMP, also plays a key role in mitochondrial lipid uptake. The role of lipid transport in mitochondria-lysosome or mitochondria-ER communication in our experimental settings is an open question, supported by the fact that iron supplementation does not fully rescue mitochondrial respiration under loss of lysosomal acidification.

OPEN QUESTIONS

In mammals, most of the reports have shown that OPA1 is the main substrate of OMA1. Our data showed that Baf A1 does not induce changes in L-OPA1

or S-OPA1 forms, indicating that an unknown substrate is responsible for this phenotype. The identity of this protein is currently under study.

OMA1 regulates glutamine incorporation into the TCA cycle. At the same time, OMA1 is necessary to sustain cell viability under loss of lysosomal acidification. Future experiments are necessary to determine the relation between the pro-survival role of OMA1 and glutamine metabolism.

Iron supplementation does fully rescue cell viability under loss of lysosomal acidification. Nevertheless, this supplementation does not fully rescue mitochondrial respiration. For one hand, that indicates that the decrease in cell viability is not due to an OXPHOS deficiency, so the cause of cell death remains unknown. In another hand, also indicates that in mammalian cells, additional molecules (e.g. metabolites), sustain mitochondria-lysosome functional communication.

CONCLUSIONS

- OMA1 is necessary to keep cell viability in conditions of endo-lysosomal V-ATPase inhibition.

- Loss of OMA1 increases the incorporation of glutamine into the TCA cycle.

- Loss of lysosomal acidification reduces the incorporation of glutamine into the TCA cycle and respiration by affecting cellular iron homeostasis

- Iron is fundamental in mitochondrial-lysosome communication

- Ang-(1-9) treatment prevents cardiomyocyte hypertrophy, mitochondrial fragmentation and loss mitochondrial-ER communication induced by NE

- Ang-(1-9) anti-hypertrophic mechanism involves the regulation of cytosolic calcium signalling, probably by keeping mitochondria-ER functional communication

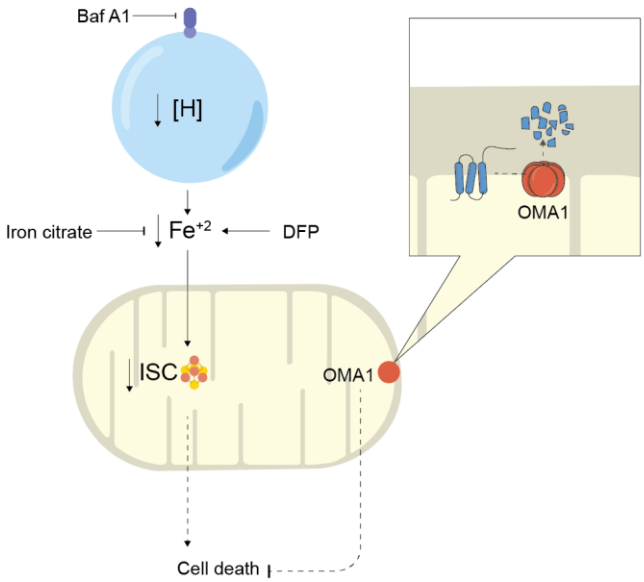

Figure 27. Model of mitochondria-lysosome communication
Endo/lysosomal v-ATPase inhibition leads to the decrease of iron availability, affecting the synthesis of iron-sulfur cluster binding proteins, reducing mitochondrial respiration. Iron supplementation rescues all these effects, indicating that iron plays a central role in mitochondria-lysosome communication. In these conditions, OMA1 plays a novel pro-survival role by regulating a yet unknown substrate.

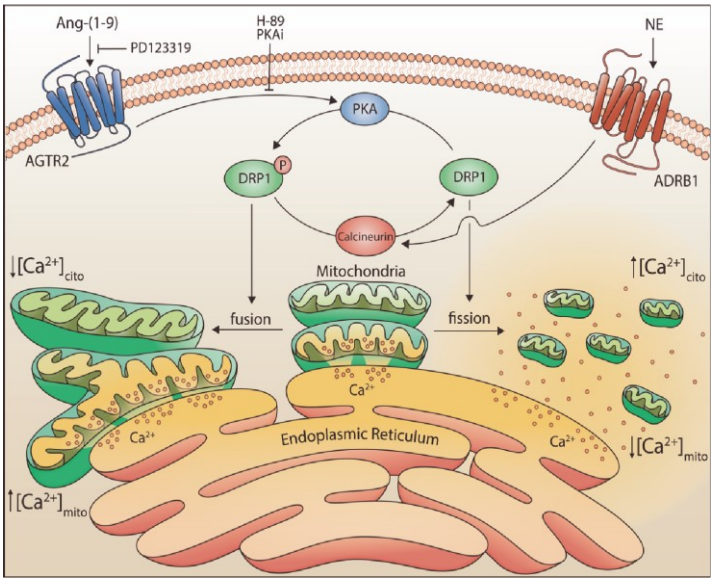

Figure 28. Model mitochondria-ER communication
Norepinephrine (NE) induces cardiomyocyte hypertrophy by inducing mitochondrial fragmentation and loss mitochondria-ER communication. Angiotensin-(1-9) treatment prevent both mitochondrial fission and loss of mitochondrial-ER communication by regulating PKA signalling pathway, preventing the increase of cytosolic calcium **(93)**.

BIBLIOGRAPHY

1. MacVicar T, Langer T. OPA1 processing in cell death and disease - the long and short of it. J Cell Sci. 2016;129(12):2297-306.
2. Labbe K, Murley A, Nunnari J. Determinants and functions of mitochondrial behavior. Annu Rev Cell Dev Biol. 2014;30:357-91.
3. Vasquez-Trincado C, Garcia-Carvajal I, Pennanen C, Parra V, Hill JA, Rothermel BA, et al. Mitochondrial dynamics, mitophagy and cardiovascular disease. J Physiol. 2016;594(3):509-25.
4. Eisner V, Picard M, Hajnoczky G. Mitochondrial dynamics in adaptive and maladaptive cellular stress responses. Nat Cell Biol. 2018;20(7):755-65.
5. Chen H, Detmer SA, Ewald AJ, Griffin EE, Fraser SE, Chan DC. Mitofusins Mfn1 and Mfn2 coordinately regulate mitochondrial fusion and are essential for embryonic development. J Cell Biol. 2003;160(2):189-200.
6. Naon D, Zaninello M, Giacomello M, Varanita T, Grespi F, Lakshminaranayan S, et al. Critical reappraisal confirms that Mitofusin 2 is an endoplasmic reticulum-mitochondria tether. Proc Natl Acad Sci U S A. 2016;113(40):11249-54.
7. Filadi R, Greotti E, Turacchio G, Luini A, Pozzan T, Pizzo P. On the role of Mitofusin 2 in endoplasmic reticulum-mitochondria tethering. Proc Natl Acad Sci U S A. 2017;114(12):E2266-E7.
8. Wai T, Langer T. Mitochondrial Dynamics and Metabolic Regulation. Trends Endocrinol Metab. 2016;27(2):105-17.
9. van der Bliek AM, Shen Q, Kawajiri S. Mechanisms of mitochondrial fission and fusion. Cold Spring Harb Perspect Biol. 2013;5(6).
10. Friedman JR, Lackner LL, West M, DiBenedetto JR, Nunnari J, Voeltz GK. ER tubules mark sites of mitochondrial division. Science. 2011;334(6054):358-62.
11. Ji WK, Hatch AL, Merrill RA, Strack S, Higgs HN. Actin filaments target the oligomeric maturation of the dynamin GTPase Drp1 to mitochondrial fission sites. Elife. 2015;4:e11553.
12. Korobova F, Ramabhadran V, Higgs HN. An actin-dependent step in mitochondrial fission mediated by the ER-associated formin INF2. Science. 2013;339(6118):464-7.
13. Li S, Xu S, Roelofs BA, Boyman L, Lederer WJ, Sesaki H, et al. Transient assembly of F-actin on the outer mitochondrial membrane contributes to mitochondrial fission. J Cell Biol. 2015;208(1):109-23.
14. Yang C, Svitkina TM. Ultrastructure and dynamics of the actin-myosin II cytoskeleton during mitochondrial fission. Nat Cell Biol. 2019.
15. Delettre C, Griffoin JM, Kaplan J, Dollfus H, Lorenz B, Faivre L, et al. Mutation spectrum and splicing variants in the OPA1 gene. Hum Genet. 2001;109(6):584-91.
16. Del Dotto V, Fogazza M, Carelli V, Rugolo M, Zanna C. Eight human OPA1 isoforms, long and short: What are they for? Biochim Biophys Acta Bioenerg. 2018;1859(4):263-9.
17. Anand R, Wai T, Baker MJ, Kladt N, Schauss AC, Rugarli E, et al. The i-AAA protease YME1L and OMA1 cleave OPA1 to balance mitochondrial fusion and fission. J Cell Biol. 2014;204(6):919-29.
18. Del Dotto V, Mishra P, Vidoni S, Fogazza M, Maresca A, Caporali L, et al. OPA1 Isoforms in the Hierarchical Organization of Mitochondrial Functions. Cell Rep. 2017;19(12):2557-71.
19. Lee H, Smith SB, Yoon Y. The short variant of the mitochondrial dynamin OPA1 maintains mitochondrial energetics and cristae structure. J Biol Chem. 2017;292(17):7115-30.

20. Quiros PM, Ramsay AJ, Sala D, Fernandez-Vizarra E, Rodriguez F, Peinado JR, et al. Loss of mitochondrial protease OMA1 alters processing of the GTPase OPA1 and causes obesity and defective thermogenesis in mice. EMBO J. 2012;31(9):2117-33.
21. Kaser M, Kambacheld M, Kisters-Woike B, Langer T. Oma1, a novel membrane-bound metallopeptidase in mitochondria with activities overlapping with the m-AAA protease. J Biol Chem. 2003;278(47):46414-23.
22. Khalimonchuk O, Jeong MY, Watts T, Ferris E, Winge DR. Selective Oma1 protease-mediated proteolysis of Cox1 subunit of cytochrome oxidase in assembly mutants. J Biol Chem. 2012;287(10):7289-300.
23. Baker MJ, Lampe PA, Stojanovski D, Korwitz A, Anand R, Tatsuta T, et al. Stress-induced OMA1 activation and autocatalytic turnover regulate OPA1-dependent mitochondrial dynamics. EMBO J. 2014;33(6):578-93.
24. Zhang K, Li H, Song Z. Membrane depolarization activates the mitochondrial protease OMA1 by stimulating self-cleavage. EMBO Rep. 2014;15(5):576-85.
25. Tulli S, Del Bondio A, Baderna V, Mazza D, Codazzi F, Pierson TM, et al. Pathogenic variants in the AFG3L2 proteolytic domain cause SCA28 through haploinsufficiency and proteostatic stress-driven OMA1 activation. J Med Genet. 2019.
26. Korwitz A, Merkwirth C, Richter-Dennerlein R, Troder SE, Sprenger HG, Quiros PM, et al. Loss of OMA1 delays neurodegeneration by preventing stress-induced OPA1 processing in mitochondria. J Cell Biol. 2016;212(2):157-66.
27. Wai T, Garcia-Prieto J, Baker MJ, Merkwirth C, Benit P, Rustin P, et al. Imbalanced OPA1 processing and mitochondrial fragmentation cause heart failure in mice. Science. 2015;350(6265):aad0116.
28. Bohovych I, Donaldson G, Christianson S, Zahayko N, Khalimonchuk O. Stress-triggered activation of the metalloprotease Oma1 involves its C-terminal region and is important for mitochondrial stress protection in yeast. J Biol Chem. 2014;289(19):13259-72.
29. Acin-Perez R, Lechuga-Vieco AV, Del Mar Munoz M, Nieto-Arellano R, Torroja C, Sanchez-Cabo F, et al. Ablation of the stress protease OMA1 protects against heart failure in mice. Sci Transl Med. 2018;10(434).
30. Sprenger HG, Wani G, Hesseling A, Konig T, Patron M, MacVicar T, et al. Loss of the mitochondrial i-AAA protease YME1L leads to ocular dysfunction and spinal axonopathy. EMBO Mol Med. 2019;11(1).
31. Scorrano L, Ashiya M, Buttle K, Weiler S, Oakes SA, Mannella CA, et al. A distinct pathway remodels mitochondrial cristae and mobilizes cytochrome c during apoptosis. Dev Cell. 2002;2(1):55-67.
32. Pernas L, Scorrano L. Mito-Morphosis: Mitochondrial Fusion, Fission, and Cristae Remodeling as Key Mediators of Cellular Function. Annu Rev Physiol. 2016;78:505-31.
33. Frezza C, Cipolat S, Martins de Brito O, Micaroni M, Beznoussenko GV, Rudka T, et al. OPA1 controls apoptotic cristae remodeling independently from mitochondrial fusion. Cell. 2006;126(1):177-89.
34. Xiao X, Hu Y, Quiros PM, Wei Q, Lopez-Otin C, Dong Z. OMA1 mediates OPA1 proteolysis and mitochondrial fragmentation in experimental models of ischemic kidney injury. Am J Physiol Renal Physiol. 2014;306(11):F1318-26.
35. Gordaliza-Alaguero I, Canto C, Zorzano A. Metabolic implications of organelle-mitochondria communication. EMBO Rep. 2019;20(9):e47928.
36. Honscher C, Mari M, Auffarth K, Bohnert M, Griffith J, Geerts W, et al. Cellular metabolism regulates contact sites between vacuoles and mitochondria. Dev Cell. 2014;30(1):86-94.

37. Elbaz-Alon Y, Rosenfeld-Gur E, Shinder V, Futerman AH, Geiger T, Schuldiner M. A Dynamic Interface between Vacuoles and Mitochondria in Yeast. Developmental Cell. 2014;30(1):95-102.
38. Lopez-Otin C, Blasco MA, Partridge L, Serrano M, Kroemer G. The hallmarks of aging. Cell. 2013;153(6):1194-217.
39. Wang Y, Hekimi S. Mitochondrial dysfunction and longevity in animals: Untangling the knot. Science. 2015;350(6265):1204-7.
40. Hughes AL, Gottschling DE. An early age increase in vacuolar pH limits mitochondrial function and lifespan in yeast. Nature. 2012;492(7428):261-5.
41. Plotegher N, Duchen MR. Mitochondrial Dysfunction and Neurodegeneration in Lysosomal Storage Disorders. Trends Mol Med. 2017;23(2):116-34.
42. Demers-Lamarche J, Guillebaud G, Tlili M, Todkar K, Belanger N, Grondin M, et al. Loss of Mitochondrial Function Impairs Lysosomes. J Biol Chem. 2016;291(19):10263-76.
43. Fernandez-Mosquera L, Yambire KF, Couto R, Pereyra L, Pabis K, Ponsford AH, et al. Mitochondrial respiratory chain deficiency inhibits lysosomal hydrolysis. Autophagy. 2019;15(9):1572-91.
44. Baixauli F, Acin-Perez R, Villarroya-Beltri C, Mazzeo C, Nunez-Andrade N, Gabande-Rodriguez E, et al. Mitochondrial Respiration Controls Lysosomal Function during Inflammatory T Cell Responses. Cell Metab. 2015;22(3):485-98.
45. Bravo-Sagua R, Rodriguez AE, Kuzmicic J, Gutierrez T, Lopez-Crisosto C, Quiroga C, et al. Cell death and survival through the endoplasmic reticulum-mitochondrial axis. Curr Mol Med. 2013;13(2):317-29.
46. Baughman JM, Perocchi F, Girgis HS, Plovanich M, Belcher-Timme CA, Sancak Y, et al. Integrative genomics identifies MCU as an essential component of the mitochondrial calcium uniporter. Nature. 2011;476(7360):341-5.
47. De Stefani D, Raffaello A, Teardo E, Szabo I, Rizzuto R. A forty-kilodalton protein of the inner membrane is the mitochondrial calcium uniporter. Nature. 2011;476(7360):336-40.
48. Patron M, Checchetto V, Raffaello A, Teardo E, Vecellio Reane D, Mantoan M, et al. MICU1 and MICU2 finely tune the mitochondrial Ca2+ uniporter by exerting opposite effects on MCU activity. Mol Cell. 2014;53(5):726-37.
49. Csordas G, Varnai P, Golenar T, Roy S, Purkins G, Schneider TG, et al. Imaging Interorganelle Contacts and Local Calcium Dynamics at the ER-Mitochondrial Interface. Molecular Cell. 2010;39(1):121-32.
50. Rizzuto R, Brini M, Murgia M, Pozzan T. Microdomains with high Ca2+ close to IP3-sensitive channels that are sensed by neighboring mitochondria. Science. 1993;262(5134):744-7.
51. Rizzuto R, Pinton P, Carrington W, Fay FS, Fogarty KE, Lifshitz LM, et al. Close contacts with the endoplasmic reticulum as determinants of mitochondrial Ca2+ responses. Science. 1998;280(5370):1763-6.
52. Bassani RA, Bassani JW, Bers DM. Mitochondrial and sarcolemmal Ca2+ transport reduce [Ca2+]i during caffeine contractures in rabbit cardiac myocytes. J Physiol. 1992;453:591-608.
53. Negretti N, O'Neill SC, Eisner DA. The relative contributions of different intracellular and sarcolemmal systems to relaxation in rat ventricular myocytes. Cardiovasc Res. 1993;27(10):1826-30.
54. Szalai G, Csordas G, Hantash BM, Thomas AP, Hajnoczky G. Calcium signal transmission between ryanodine receptors and mitochondria. J Biol Chem. 2000;275(20):15305-13.

55. Drago I, De Stefani D, Rizzuto R, Pozzan T. Mitochondrial Ca2+ uptake contributes to buffering cytoplasmic Ca2+ peaks in cardiomyocytes. Proc Natl Acad Sci U S A. 2012;109(32):12986-91.
56. Hill JA, Olson EN. Cardiac plasticity. N Engl J Med. 2008;358(13):1370-80.
57. Burchfield JS, Xie M, Hill JA. Pathological ventricular remodeling: mechanisms: part 1 of 2. Circulation. 2013;128(4):388-400.
58. Gutierrez T, Parra V, Troncoso R, Pennanen C, Contreras-Ferrat A, Vasquez-Trincado C, et al. Alteration in mitochondrial Ca(2+) uptake disrupts insulin signaling in hypertrophic cardiomyocytes. Cell Commun Signal. 2014;12:68.
59. Pennanen C, Parra V, Lopez-Crisosto C, Morales PE, Del Campo A, Gutierrez T, et al. Mitochondrial fission is required for cardiomyocyte hypertrophy mediated by a Ca2+-calcineurin signaling pathway. J Cell Sci. 2014;127(Pt 12):2659-71.
60. Donoghue M, Hsieh F, Baronas E, Godbout K, Gosselin M, Stagliano N, et al. A novel angiotensin-converting enzyme-related carboxypeptidase (ACE2) converts angiotensin I to angiotensin 1-9. Circ Res. 2000;87(5):E1-9.
61. Flores-Munoz M, Work LM, Douglas K, Denby L, Dominiczak AF, Graham D, et al. Angiotensin-(1-9) attenuates cardiac fibrosis in the stroke-prone spontaneously hypertensive rat via the angiotensin type 2 receptor. Hypertension. 2012;59(2):300-7.
62. Flores-Munoz M, Smith NJ, Haggerty C, Milligan G, Nicklin SA. Angiotensin1-9 antagonises pro-hypertrophic signalling in cardiomyocytes via the angiotensin type 2 receptor. J Physiol. 2011;589(Pt 4):939-51.
63. Ocaranza MP, Lavandero S, Jalil JE, Moya J, Pinto M, Novoa U, et al. Angiotensin-(1-9) regulates cardiac hypertrophy in vivo and in vitro. J Hypertens. 2010;28(5):1054-64.
64. Yoshimori T, Yamamoto A, Moriyama Y, Futai M, Tashiro Y. Bafilomycin A1, a specific inhibitor of vacuolar-type H(+)-ATPase, inhibits acidification and protein degradation in lysosomes of cultured cells. J Biol Chem. 1991;266(26):17707-12.
65. Grootjans S, Hassannia B, Delrue I, Goossens V, Wiernicki B, Dondelinger Y, et al. A real-time fluorometric method for the simultaneous detection of cell death type and rate. Nat Protoc. 2016;11(8):1444-54.
66. Tewari M, Quan LT, Orourke K, Desnoyers S, Zeng Z, Beidler DR, et al. Yama/Cpp32-Beta, a Mammalian Homolog of Ced-3, Is a Crma-Inhibitable Protease That Cleaves the Death Substrate Poly(Adp-Ribose) Polymerase. Cell. 1995;81(5):801-9.
67. Galluzzi L, Aaronson SA, Abrams J, Alnemri ES, Andrews DW, Baehrecke EH, et al. Guidelines for the use and interpretation of assays for monitoring cell death in higher eukaryotes. Cell Death Differ. 2009;16(8):1093-107.
68. Mauvezin C, Nagy P, Juhasz G, Neufeld TP. Autophagosome-lysosome fusion is independent of V-ATPase-mediated acidification. Nat Commun. 2015;6:7007.
69. Palikaras K, Lionaki E, Tavernarakis N. Mechanisms of mitophagy in cellular homeostasis, physiology and pathology. Nat Cell Biol. 2018;20(9):1013-22.
70. Medeiros TC, Thomas RL, Ghillebert R, Graef M. Autophagy balances mtDNA synthesis and degradation by DNA polymerase POLG during starvation. J Cell Biol. 2018;217(5):1601-11.
71. Hurley JH, Young LN. Mechanisms of Autophagy Initiation. Annu Rev Biochem. 2017;86:225-44.
72. Kaushik S, Cuervo AM. The coming of age of chaperone-mediated autophagy. Nat Rev Mol Cell Biol. 2018;19(6):365-81.
73. Klionsky DJ, Abdelmohsen K, Abe A, Abedin MJ, Abeliovich H, Acevedo Arozena A, et al. Guidelines for the use and interpretation of assays for monitoring autophagy (3rd edition). Autophagy. 2016;12(1):1-222.

74. Huss M, Ingenhorst G, Konig S, Gassel M, Drose S, Zeeck A, et al. Concanamycin A, the specific inhibitor of V-ATPases, binds to the V(o) subunit c. J Biol Chem. 2002;277(43):40544-8.
75. Elliott IA, Dann AM, Xu S, Kim SS, Abt ER, Kim W, et al. Lysosome inhibition sensitizes pancreatic cancer to replication stress by aspartate depletion. Proc Natl Acad Sci U S A. 2019;116(14):6842-7.
76. Abu-Remaileh M, Wyant GA, Kim C, Laqtom NN, Abbasi M, Chan SH, et al. Lysosomal metabolomics reveals V-ATPase- and mTOR-dependent regulation of amino acid efflux from lysosomes. Science. 2017;358(6364):807-+.
77. Cluntun AA, Lukey MJ, Cerione RA, Locasale JW. Glutamine Metabolism in Cancer: Understanding the Heterogeneity. Trends Cancer. 2017;3(3):169-80.
78. Zhang J, Pavlova NN, Thompson CB. Cancer cell metabolism: the essential role of the nonessential amino acid, glutamine. Embo Journal. 2017;36(10):1302-15.
79. DeBerardinis RJ, Mancuso A, Daikhin E, Nissim I, Yudkoff M, Wehrli S, et al. Beyond aerobic glycolysis: Transformed cells can engage in glutamine metabolism that exceeds the requirement for protein and nucleotide synthesis. P Natl Acad Sci USA. 2007;104(49):19345-50.
80. Gaude E, Schmidt C, Gammage PA, Dugourd A, Blacker T, Chew SP, et al. NADH Shuttling Couples Cytosolic Reductive Carboxylation of Glutamine with Glycolysis in Cells with Mitochondrial Dysfunction. Mol Cell. 2018;69(4):581-93 e7.
81. Mullen AR, Wheaton WW, Jin ES, Chen PH, Sullivan LB, Cheng T, et al. Reductive carboxylation supports growth in tumour cells with defective mitochondria. Nature. 2011;481(7381):385-8.
82. Bezawork-Geleta A, Rohlena J, Dong LF, Pacak K, Neuzil J. Mitochondrial Complex II: At the Crossroads. Trends Biochem Sci. 2017;42(4):312-25.
83. Lane DJ, Merlot AM, Huang ML, Bae DH, Jansson PJ, Sahni S, et al. Cellular iron uptake, trafficking and metabolism: Key molecules and mechanisms and their roles in disease. Biochim Biophys Acta. 2015;1853(5):1130-44.
84. Bogdan AR, Miyazawa M, Hashimoto K, Tsuji Y. Regulators of Iron Homeostasis: New Players in Metabolism, Cell Death, and Disease. Trends Biochem Sci. 2016;41(3):274-86.
85. Miles AL, Burr SP, Grice GL, Nathan JA. The vacuolar-ATPase complex and assembly factors, TMEM199 and CCDC115, control HIF1alpha prolyl hydroxylation by regulating cellular iron levels. Elife. 2017;6.
86. Li HH, Zhao HT, Hao SY, Shang LC, Wu J, Song CH, et al. Iron regulatory protein deficiency compromises mitochondrial function in murine embryonic fibroblasts. Sci Rep-Uk. 2018;8.
87. Na U, Yu WD, Cox J, Bricker DK, Brockmann K, Rutter J, et al. The LYR Factors SDHAF1 and SDHAF3 Mediate Maturation of the Iron-Sulfur Subunit of Succinate Dehydrogenase. Cell Metabolism. 2014;20(2):253-66.
88. Maio N, Ghezzi D, Verrigni D, Rizza T, Bertini E, Martinelli D, et al. Disease-Causing SDHAF1 Mutations Impair Transfer of Fe-S Clusters to SDHB. Cell Metabolism. 2016;23(2):292-302.
89. Erlitzki R, Long JC, Theil EC. Multiple, conserved iron-responsive elements in the 3'-untranslated region of transferrin receptor mRNA enhance binding of iron regulatory protein 2. J Biol Chem. 2002;277(45):42579-87.
90. Lill R, Freibert SA. Mechanisms of Mitochondrial Iron-Sulfur Protein Biogenesis. Annu Rev Biochem. 2020.
91. Fattah C, Nather K, McCarroll CS, Hortigon-Vinagre MP, Zamora V, Flores-Munoz M, et al. Gene Therapy With Angiotensin-(1-9) Preserves Left Ventricular Systolic Function After Myocardial Infarction. J Am Coll Cardiol. 2016;68(24):2652-66.

92. Mendoza-Torres E, Riquelme JA, Vielma A, Sagredo AR, Gabrielli L, Bravo-Sagua R, et al. Protection of the myocardium against ischemia/reperfusion injury by angiotensin-(1-9) through an AT2R and Akt-dependent mechanism. Pharmacol Res. 2018;135:112-21.
93. Sotomayor-Flores C, Rivera-Mejias P, Vasquez-Trincado C, Lopez-Crisosto C, Morales PE, Pennanen C, et al. Angiotensin-(1-9) prevents cardiomyocyte hypertrophy by controlling mitochondrial dynamics via miR-129-3p/PKIA pathway. Cell Death Differ. 2020.
94. Colella M, Grisan F, Robert V, Turner JD, Thomas AP, Pozzan T. Ca2+ oscillation frequency decoding in cardiac cell hypertrophy: role of calcineurin/NFAT as Ca2+ signal integrators. Proc Natl Acad Sci U S A. 2008;105(8):2859-64.
95. Yang J, Rothermel B, Vega RB, Frey N, McKinsey TA, Olson EN, et al. Independent signals control expression of the calcineurin inhibitory proteins MCIP1 and MCIP2 in striated muscles. Circ Res. 2000;87(12):E61-8.
96. Choi AM, Ryter SW, Levine B. Autophagy in human health and disease. N Engl J Med. 2013;368(19):1845-6.
97. Luzio JP, Parkinson MDJ, Gray SR, Bright NA. The delivery of endocytosed cargo to lysosomes. Biochem Soc T. 2009;37:1019-21.
98. Lim CY, Zoncu R. The lysosome as a command-and-control center for cellular metabolism. Journal of Cell Biology. 2016;214(6):653-64.
99. Platt FM, Boland B, van der Spoel AC. Lysosomal storage disorders: The cellular impact of lysosomal dysfunction. Journal of Cell Biology. 2012;199(5):723-34.
100. Li SC, Kane PM. The yeast lysosome-like vacuole: Endpoint and crossroads. Bba-Mol Cell Res. 2009;1793(4):650-63.
101. Ducker GS, Rabinowitz JD. One-Carbon Metabolism in Health and Disease. Cell Metab. 2017;25(1):27-42.
102. Bricker DK, Taylor EB, Schell JC, Orsak T, Boutron A, Chen YC, et al. A Mitochondrial Pyruvate Carrier Required for Pyruvate Uptake in Yeast, Drosophila, and Humans. Science. 2012;337(6090):96-100.
103. Vacanti NM, Divakaruni AS, Green CR, Parker SJ, Henry RR, Ciaraldi TP, et al. Regulation of Substrate Utilization by the Mitochondrial Pyruvate Carrier. Molecular Cell. 2014;56(3):425-35.
104. Yang CD, Ko B, Hensley CT, Jiang L, Wasti AT, Kim J, et al. Glutamine Oxidation Maintains the TCA Cycle and Cell Survival during Impaired Mitochondrial Pyruvate Transport. Molecular Cell. 2014;56(3):414-24.
105. Hughes CE, Coody TK, Jeong MY, Berg JA, Winge DR, Hughes AL. Cysteine Toxicity Drives Age-Related Mitochondrial Decline by Altering Iron Homeostasis. Cell. 2020;180(2):296-310 e18.
106. Weber RA, Yen FS, Nicholson SPV, Alwaseem H, Bayraktar EC, Alam M, et al. Maintaining Iron Homeostasis Is the Key Role of Lysosomal Acidity for Cell Proliferation. Mol Cell. 2020;77(3):645-55 e7.
107. Yambire KF, Rostosky C, Watanabe T, Pacheu-Grau D, Torres-Odio S, Sanchez-Guerrero A, et al. Impaired lysosomal acidification triggers iron deficiency and inflammation in vivo. Elife. 2019;8.
108. Sheftel AD, Zhang AS, Brown C, Shirihai OS, Ponka P. Direct interorganellar transfer of iron from endosome to mitochondrion. Blood. 2006;108(11):83a-a.
109. Das A, Nag S, Mason AB, Barroso MM. Endosome-mitochondria interactions are modulated by iron release from transferrin. Journal of Cell Biology. 2016;214(7):831-45.
110. Lopez-Crisosto C, Pennanen C, Vasquez-Trincado C, Morales P, Bravo-Sagua R, Quest AFG, et al. Sarcoplasmic reticulum-mitochondria communication in cardiovascular pathophysiology. Nat Rev Cardiol. 2017;14(6):342-60.

111. Eisner V, Parra V, Lavandero S, Hidalgo C, Jaimovich E. Mitochondria fine-tune the slow Ca(2+) transients induced by electrical stimulation of skeletal myotubes. Cell Calcium. 2010;48(6):358-70.
112. Kowaltowski AJ, Menezes SL, Assali EA, Goncalves IG, Cabral-Costa JV, Abreu P, et al. Mitochondrial morphology regulates organellar Ca2+ uptake and changes cellular Ca2+ homeostasis. Faseb Journal. 2019;33(12):13176-88.
113. Parra V, Rothermel BA. Calcineurin signaling in the heart: The importance of time and place. J Mol Cell Cardiol. 2017;103:121-36.